Supporting Information

Decoding the Fucose Migration Product during Mass-Spectrometric analysis of Blood Group Epitopes

Maike Lettow[1,2], Kim Greis[1,2], Eike Mucha[1], Tyler R. Lambeth[5], Murat Yaman[3,4], Vasilis Kontodimas[3], Christian Manz[1,2], Waldemar Hoffmann[1,2], Gerard Meijer[1], Ryan R. Julian[5], Gert von Helden[1], Mateusz Marianski*[3,4], and Kevin Pagel*[1,2]

[1]Fritz-Haber-Intitut der Max-Planck-Gesellschaft

[2]Institute of Chemistry and Biochemistry, Freie Universität Berlin

[3]Department of Chemistry and Biochemistry, Hunter College, The City University of New York

[4]The PhD Program in Chemistry and Biochemistry, The Graduate Center, The City University of New York

[5]Department of Chemistry, University of California, Riverside

Table of Contents:

Sample Preparation

Commercially available Lewis and blood group antigens, solvents (HPLC grade) and chemicals for glycan modification were purchased and used without further purification from Dextra Laboratories (UK) and Sigma-Aldrich (USA), respectively. Aqueous glycan stock solutions (1 mM and 100 µM for glycans with linker) were freshly diluted with water/methanol (*v/v*, 50/50) to yield 50 µM analyte solutions prior their analysis.

The spectra are measured in the 1000-1800 cm^{-1} range using a step size of 2 cm^{-1}. Every ion, and using each trap, is measured at least twice. The laser power is fitted using a polynomial regression function (4^{th} degree) and the ion signal is divided by the obtained function as a linear power correction. Then, corrected spectra of an ion are normalized and averaged leading to the final spectra shown in this work. The two spectra of $[BG\text{-}H2+H]^+$ in the warm trap, which shows the reproducibility of the method, are shown in Figure S3.

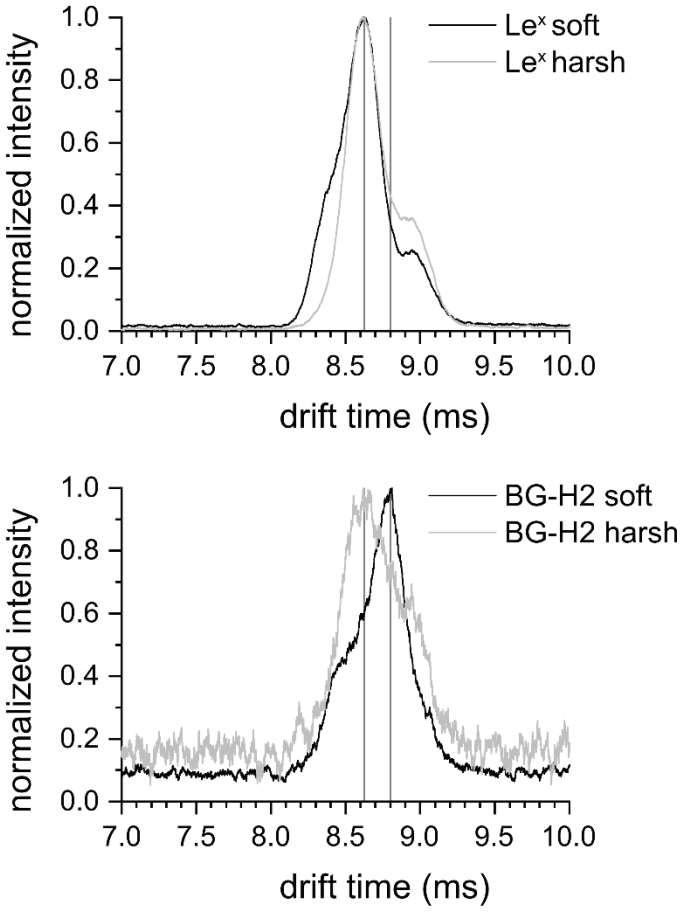

Figure S1: Arrival time distributions (ATDs) in classical plots for comparison to their representation in heatmaps of activated (harsh conditions) and non-activated (soft conditions) intact precursor standards of $[Le^x+H]^+$ and $[BG\text{-}H2+H]^+$.

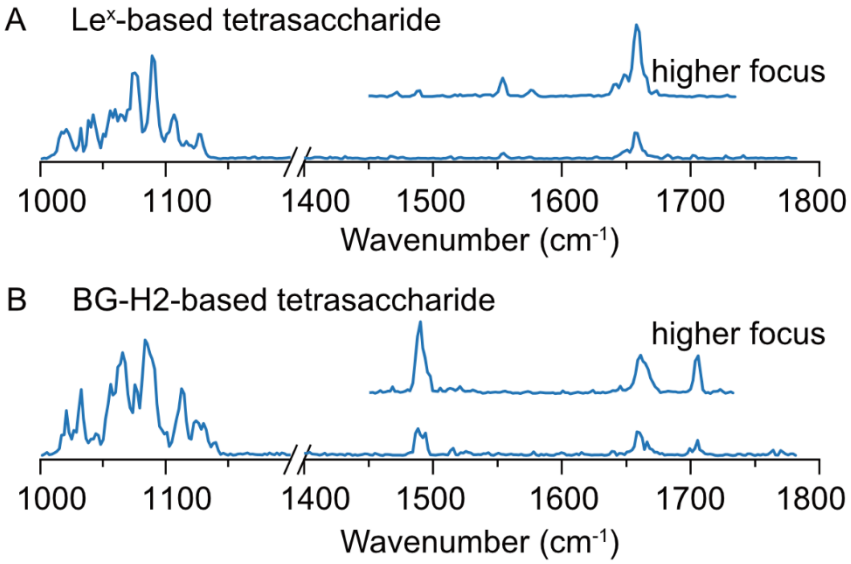

Figure S2: IR spectra of the intact (A) Le^x- and (B) BG-H2-based tetrasaccharides. The IR spectrum of the Le^x-based tetrasaccharide features a subset of vibrational bands from the IR spectrum of the BG-H2-based tetrasaccharide. As an inset, IR spectra recorded with a higher laser focus (i.e. higher photon density) are given with each spectrum to potentially resolve weaker vibrational modes.

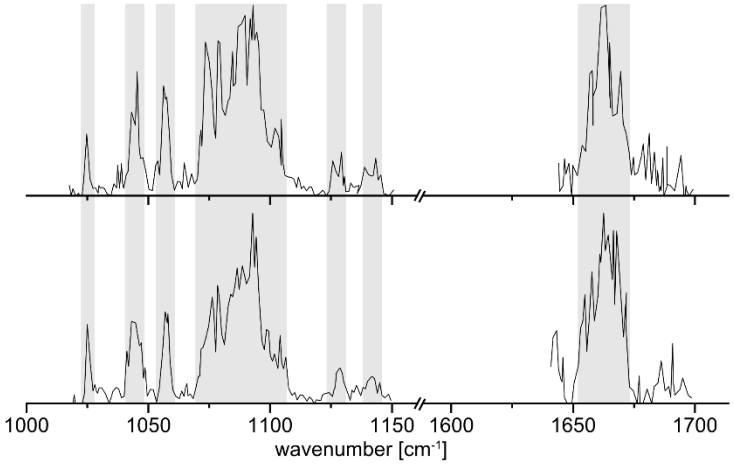

Figure S3: Two individual measurements of the IR spectra of the intact $[BG\text{-}H2+H]^+$ ion using the warm trap. The spectra show high reproducibility in the amide region. The spectra presented in the paper are the average of two measurements.

Computational Methods

The search protocol has been implemented in the CarPpy python package (manuscript in preparation). In details, we have investigated each of 64 types of linkages linkage between the fucose and the Gal$\beta(1 \rightarrow 4)$GlcNAc core in both configurations, both orientations of the amide group, and in both anomeric forms of the reducing GlcNAc. The sampling of the amide-protonated trisccharides have has been initiated from Replica-Exchange MD simulations, using CHARMM36 force field[1] and Gromacs2018.1 software,[2] to generate the initial set of unbiased structures in a temperature of 450 K. From each of these trajectories, two structures which differed by the rotation of at least one glycosidic bond were selected as the initial structure for the structural search using CREST with methods from the xTB package. The conformational search was carried out using GFN2-xTB energy function.[3] The resulting searches were merged and clustered to generate a set of initial structures for the DFT calculations. For the clustering, done with the single-linkage algorithm implemented in the scipy module, we have chosen energy-dependent RMSD criteria, where the RMSD changes from 1.0 Å for structures within 2.0 kcal mol^{-1} above the minimum, to 2.0 Å for structures within 2.0-5.0 kcal mol^{-1} energy window, to 4.0 Å for structures less stable than 5.0 kcal mol^{-1}. Only heavy atoms were included in the RMSD calculations. The selected structures were optimized using PBE0[4] hybrid functional and 6-31G(d,p) basis set in Gaussian16 RevB.01 software.[5] The number of individual optimizations is listed in Table S1, and the conformational plots are shown in Figures S4-35. The resulting structures were collected and clustered once again, using tighter geometrical criteria of 1.0, 1.5, and 2.0 Å for the same energy windows. The selected unique ions are marked in dark blue in the Figures S5-36. From these unique conformers, we selected all structures within 6.0 kcal mol^{-1} energy window (if there were less than 10, we extended the ceiling) and reoptimized them using the dispersion-corrected PBE0+D3BJ hybrid functional[4,6] and a larger 6-311+G(d,p) basis set, followed by the calculations of harmonic vibrational frequencies. The number of individual calculations has been listed in the Table S1. In addition, to improve the sampling of the two starting trissacharides, Le^x and BG-H2, the eight sets (two anomers and two amide bond orientations) were appended with structures generated from a third independent CREST search and reoptimized at the same level of theory, which resulted in additional 185 conformers distributed among these isomers (Table S1). The relaxed geometries were used for the prediction of their CCS using the projection approximation method implemented in the sigma code (hereafter referred as ^{PA}CCS).[24] Finally, for the selected structures we have computed the anharmonic IR spectra using second-order perturbative approach,[7] using harmonic modes 80-130 (range of 950 cm^{-1} to 1300 cm^{-1}). All anharmonic spectra have been redshifted 50 cm^{-1}. The amide I vibration has been evaluated using harmonic approximation and scaled using a default 0.965 scaling factor that has previously been employed for similar systems in other work. [8,9]

Table S1: Summary of the number of individual DFT optimizations in 6-31G(d,p) basis set(small basis, **SB**), and optimizations + frequency calulations in 6-311+G(d,p) basis set (large basis, **LG**). The calculations in **LB** of *Le*^{x} (red), *BG-H2* (blue) and *α16* (gray) have been appended with additional structures from a separate crest-search.

Bond configuration				*α*-anomer				*β*-anomer			
				α		*β*		*α*		*β*	
	Linkage	Amide	SNFG symbol	SB	LB	SB	LB	SB	LB	SBF	LB
GlcNAc	1-1	trans	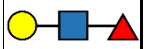	25	6	27	5	34	10	73	10
	1-1	cis		37	7	64	12	83	10	97	16
	1-2	trans		110	10	113	10	130	10	109	15
	1-2	cis		46	10	101	21	188	10	78	16
	1-3	trans		270	52	28	10	38	16	13	9
	1-3	cis		239	91	129	19	82	55	46	12
	1-6	trans		60	16	106	23	30	11	47	10
	1-6	cis		91	19	102	16	34	10	55	12
Gal	1-2	trans		22	24	44	10	57	29	116	10
	1-2	cis		108	47	45	10	23	30	43	10
	1-3	trans	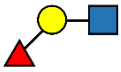	50	10	65	10	154	11	95	12
	1-3	cis		235	10	142	26	77	10	148	10
	1-4	trans		112	10	29	9	259	10	28	10
	1-4	cis		41	12	75	10	84	10	49	10
	1-6	trans	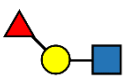	24	27	135	12	58	43	104	10
	1-6	cis		165	51	68	11	18	17	53	10

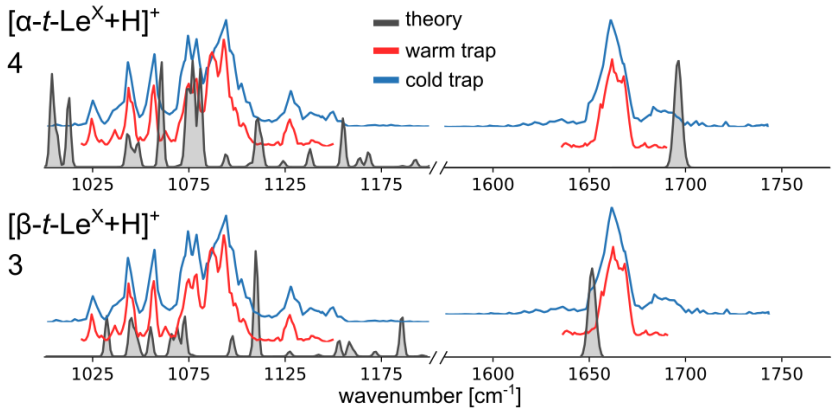

Figure S4: Simulated anharmonic IR spectra of the two most stable anomers of $[Le^x+H]^+$. The relative energies of the ions are shown in Figure 2.

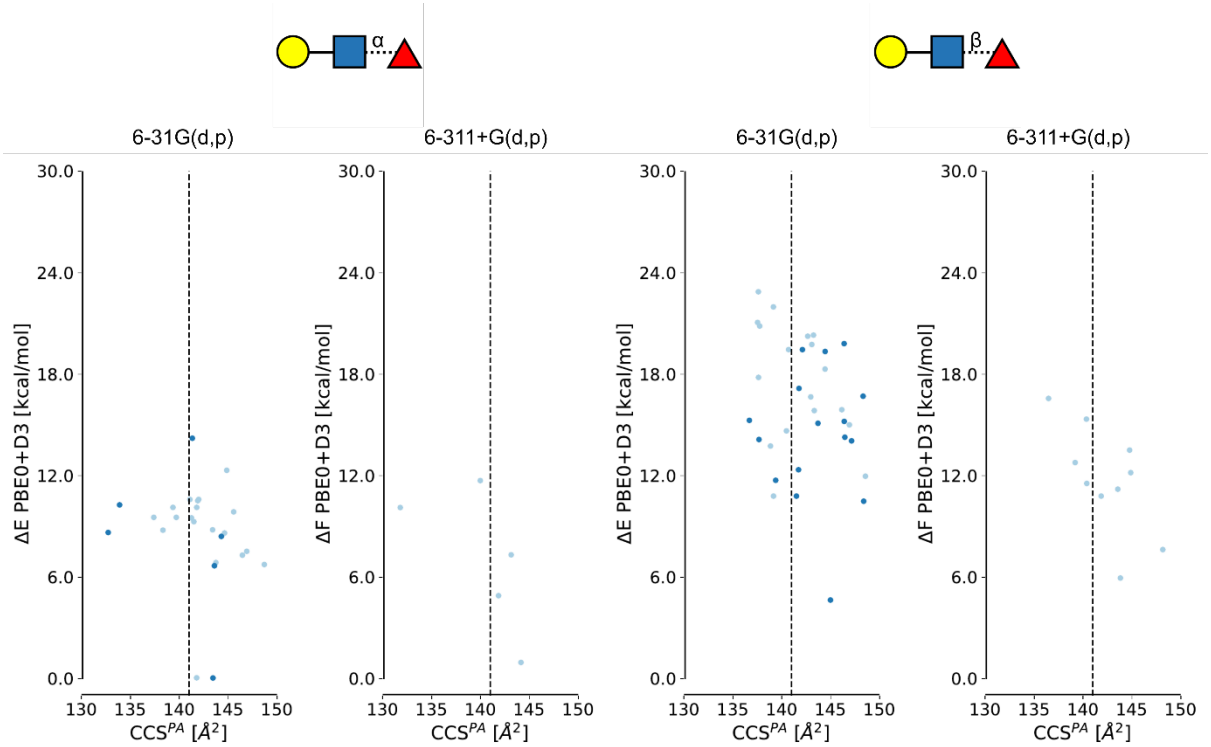

Figure S5: The CCS^{PA} vs. relative energy (ΔE, in a small 6-31G(d,p) basis set), or free-energy (ΔF, in a larger 6-311+G(d,p) basis set, evaluated at 300 K) of two anomers of the protonated **Galβ(1→4)GlcNAcα/β(1↔1)Fucα** and trans amide bond orientation. The glycan is shown above using the SNFG notation. The y-axis shows the (free-)energy relatively to the lowest (free-)energy conformer of the **[α-t-α16+H]⁺.** The dashed line represents the experimental $^{DT}CCS_{He}$. The conformers highlighted with dark blue have been selected to be reoptimized in a larger basis set.

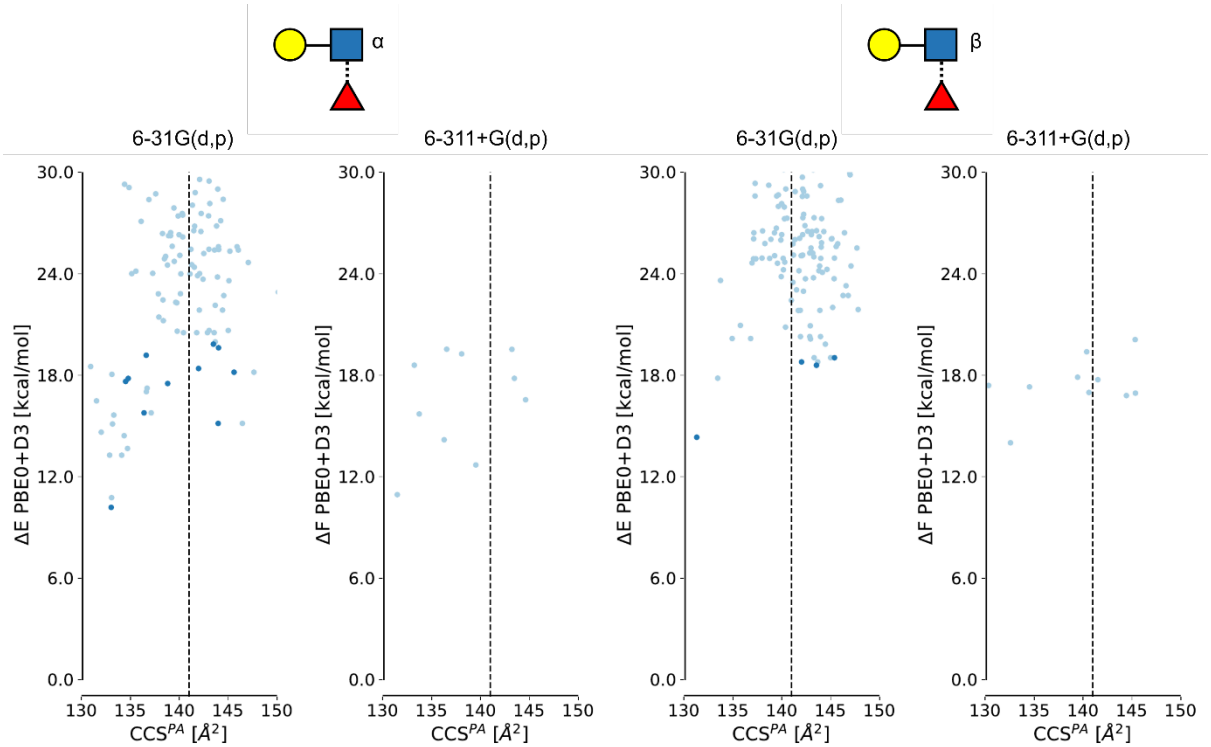

Figure S6: The CCS^{PA} vs. relative energy (ΔE, in a small 6-31G(d,p) basis set), or free-energy (ΔF, in a larger 6-311+G(d,p) basis set, evaluated at 300 K) of two anomers of the protonated **Galβ(1→4)[Fucα(1→2)]GlcNAcα/β** and trans amide bond orientation. The glycan is shown above using the SNFG notation. The y-axis shows the (free-)energy relatively to the lowest (free-)energy conformer of the **[α-t-α16+H]⁺.** The dashed line represents the experimental $^{DT}CCS_{He}$. The conformers highlighted with dark blue have been selected to be reoptimized in a larger basis set.

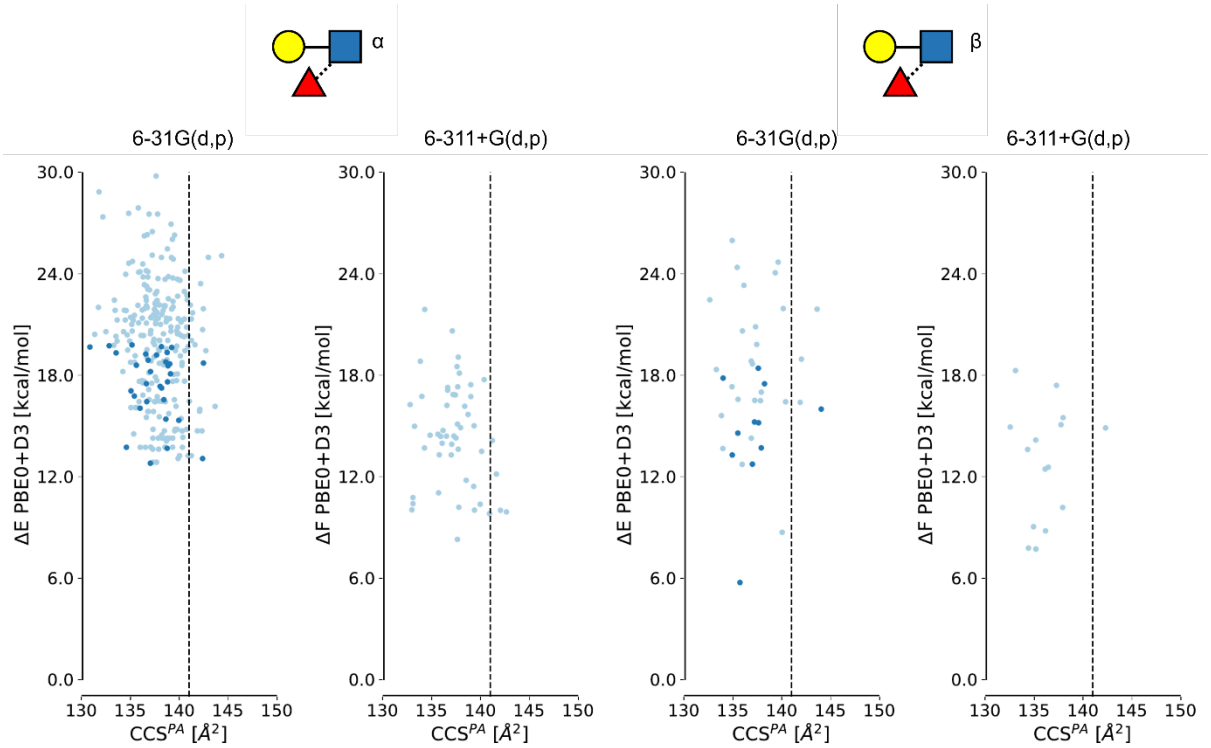

Figure S7: The CCS^{PA} vs. relative energy (ΔE, in a small 6-31G(d,p) basis set), or free-energy (ΔF, in a larger 6-311+G(d,p) basis set, evaluated at 300 K) of two anomers of the protonated **Galβ(1→4)[Fucα(1→3)]GlcNAcα/β** and trans amide bond orientation. The glycan is shown above using SNFG notation. The y-axis shows the (free-)energy relatively to the lowest (free-)energy conformer of the **[α-t-α16+H]⁺.** The dashed line represents the experimental $^{DT}CCS_{He}$. The conformers highlighted with dark blue have been selected to be reoptimized in a larger basis set.

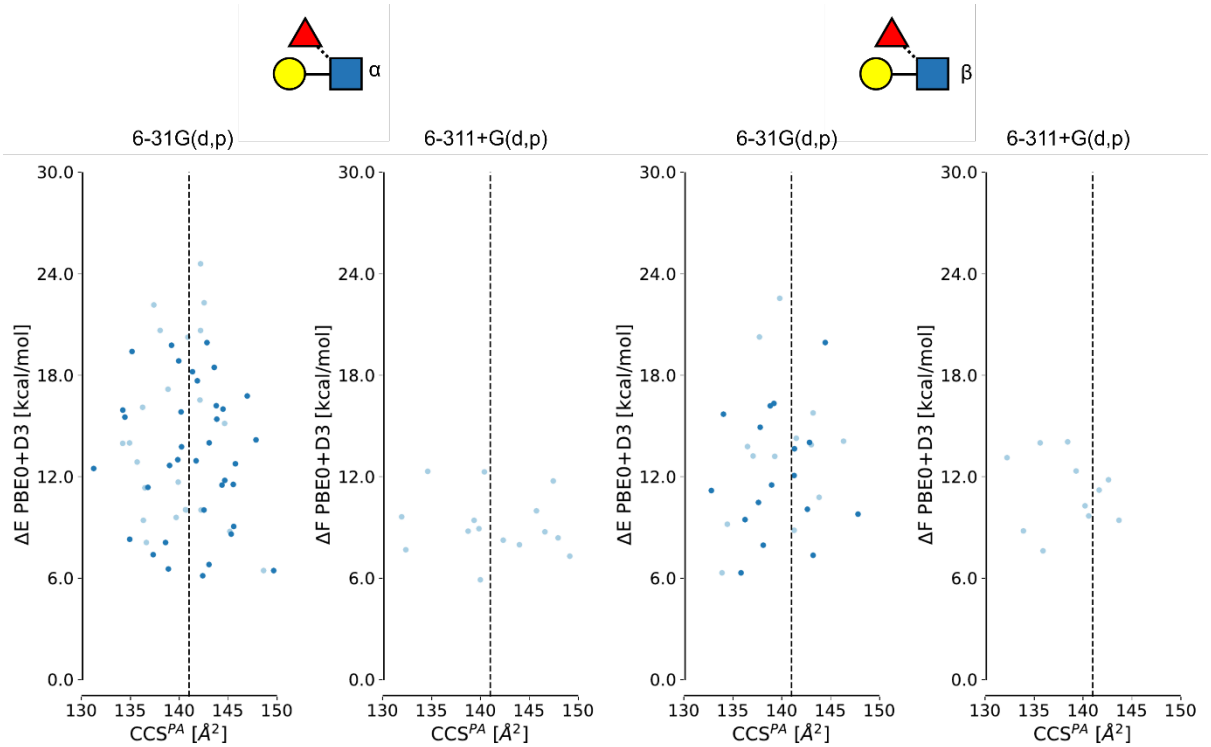

Figure S8: The CCS^{PA} vs. relative energy (ΔE, in a small 6-31G(d,p) basis set), or free-energy (ΔF, in a larger 6-311+G(d,p) basis set, evaluated at 300 K) of two anomers of the protonated **Galβ(1→4)[Fucα(1→6)]GlcNAcα/β** and trans amide bond orientation. The glycan is shown above using the SNFG notation. The y-axis shows the (free-)energy relatively to the lowest (free-)energy conformer of the **[α-t-α16+H]⁺.** The dashed line represents the experimental $^{DT}CCS_{He}$. The conformers highlighted with dark blue have been selected to be reoptimized in a larger basis set.

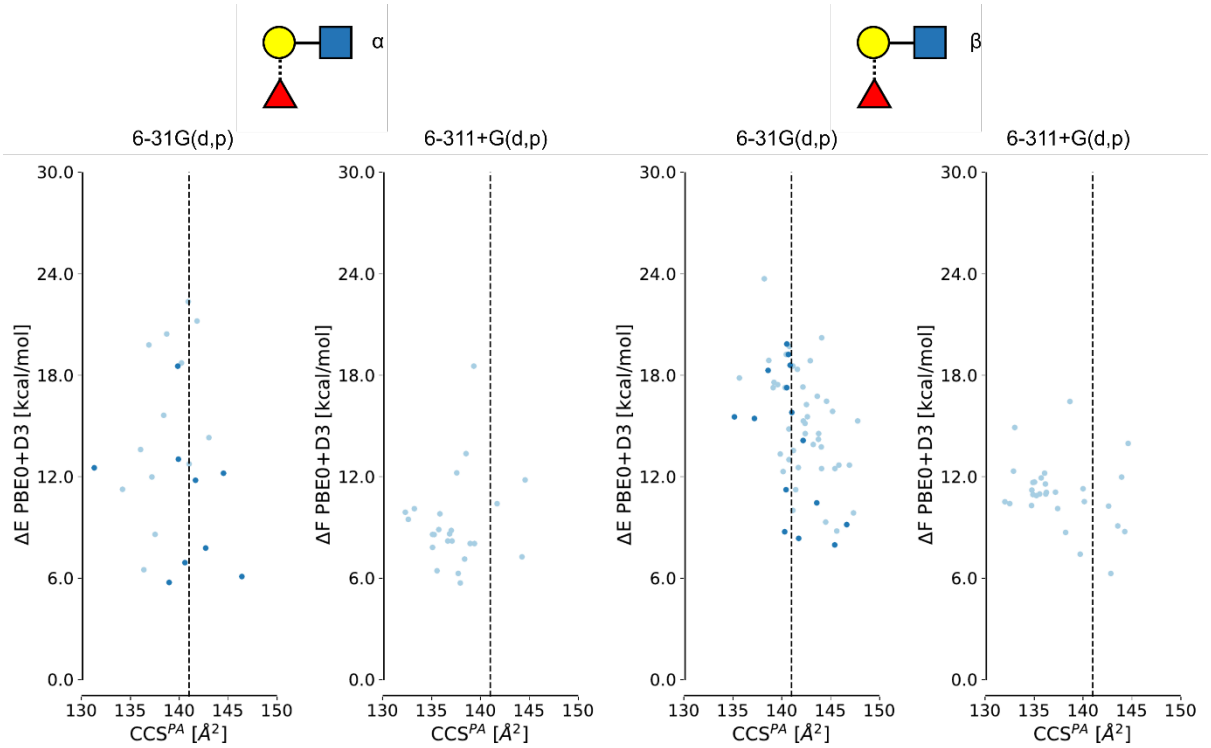

Figure S9: The CCS^{PA} vs. relative energy (ΔE, in a small 6-31G(d,p) basis set), or free-energy (ΔF, in a larger 6-311+G(d,p) basis set, evaluated at 300 K) of two anomers of the protonated **Fucα(1→2)Galβ(1→4)GlcNAcα/β** and trans amide bond orientation. The glycan is shown above using the SNFG notation. The y-axis shows the (free-)energy relatively to the lowest (free-)energy conformer of the **[α-t-α16+H]⁺.** The dashed line represents the experimental $^{DT}CCS_{He}$. The conformers highlighted with dark blue have been selected to be reoptimized in a larger basis set.

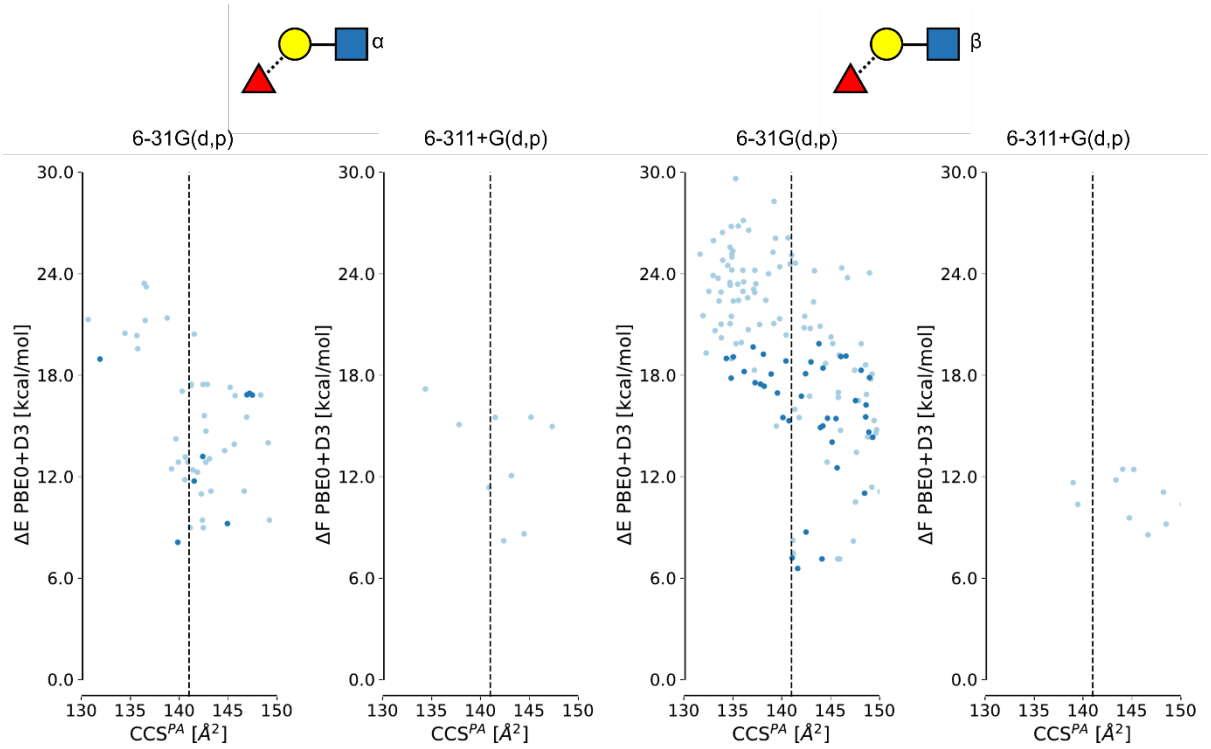

Figure S10: The CCS^{PA} vs. relative energy (ΔE, in a small 6-31G(d,p) basis set), or free-energy (ΔF, in a larger 6-311+G(d,p) basis set, evaluated at 300 K) of two anomers of the protonated **Fucα(1→3)Galβ(1→4)GlcNAcα/β** and trans amide bond orientation. The glycan is shown above using the SNFG notation. The y-axis shows the (free-)energy relatively to the lowest (free-)energy conformer of the **[α-t-α16+H]⁺.** The dashed line represents the experimental $^{DT}CCS_{He}$. The conformers highlighted with dark blue have been selected to be reoptimized in a larger basis set.

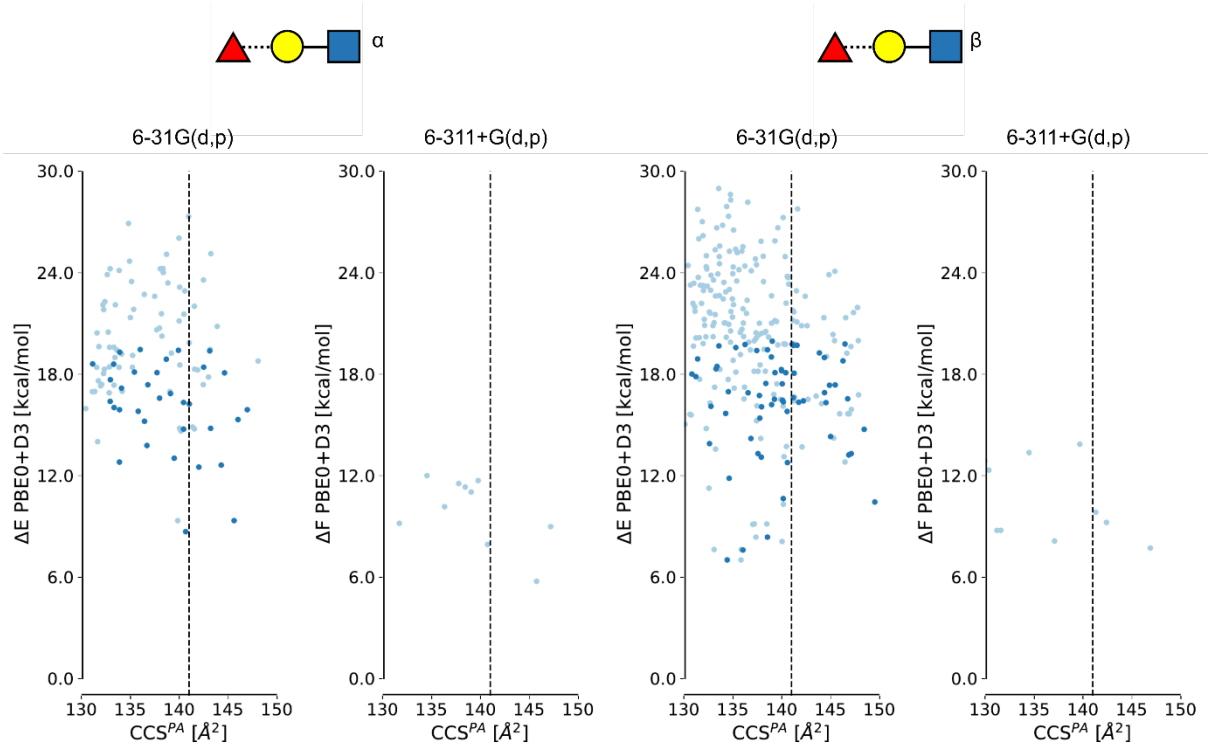

Figure S11: The CCS^{PA} vs. relative energy (ΔE, in a small 6-31G(d,p) basis set), or free-energy (ΔF, in a larger 6-311+G(d,p) basis set, evaluated at 300 K) of two anomers of the protonated **Fucα(1→4)Galβ(1→4)GlcNAcα/β** and trans amide bond orientation. The glycan is shown above using the SNFG notation. The y-axis shows the (free-)energy relatively to the lowest (free-)energy conformer of the **[α-t-α16+H]⁺.** The dashed line represents the experimental $^{DT}CCS_{He}$. The conformers highlighted with dark blue have been selected to be reoptimized in a larger basis set.

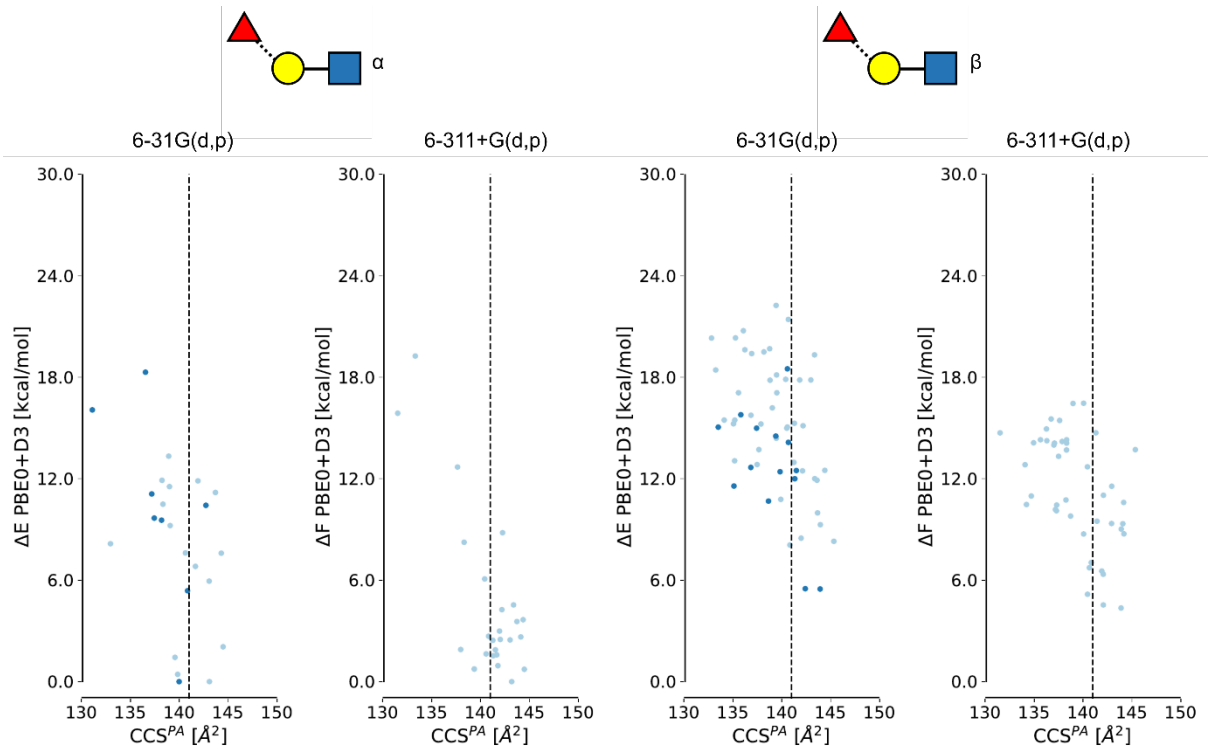

Figure S12: The CCS^{PA} vs. relative energy (ΔE, in a small 6-31G(d,p) basis set), or free-energy (ΔF, in a larger 6-311+G(d,p) basis set, evaluated at 300 K) of two anomers of the protonated **Fucα(1→6)Galβ(1→4)GlcNAcα/β** and trans amide bond orientation. The glycan is shown above using the SNFG notation. The y-axis shows the (free-)energy relatively to the lowest (free-)energy conformer of the **[α-t-α16+H]⁺.** The dashed line represents the experimental $^{DT}CCS_{He}$. The conformers highlighted with dark blue have been selected to be reoptimized in a larger basis set.

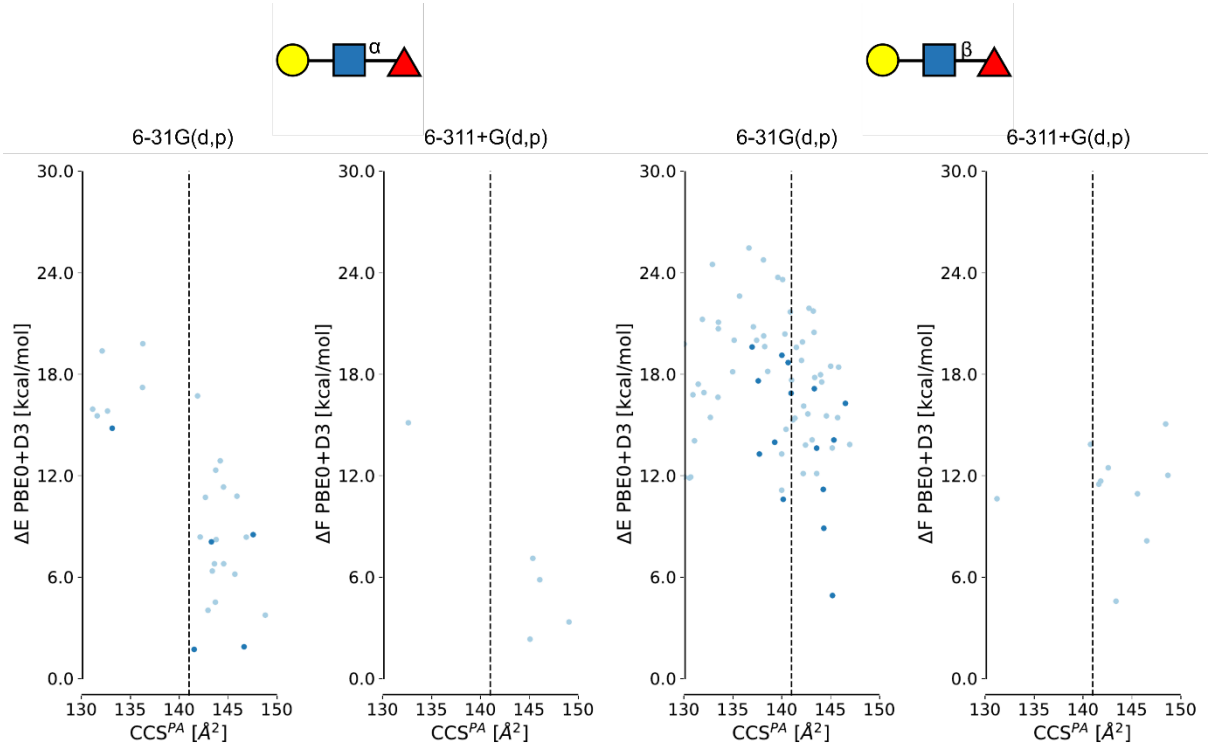

Figure S13: The CCS^{PA} vs. relative energy (ΔE, in a small 6-31G(d,p) basis set), or free-energy (ΔF, in a larger 6-311+G(d,p) basis set, evaluated at 300 K) of two anomers of the protonated **Galβ(1→4)GlcNAcα/β(1↔1)Fucβ** and trans amide bond orientation. The glycan is shown above using the SNFG notation. The y-axis shows the (free-)energy relatively to the lowest (free-)energy conformer of the **[α-t-α16+H]⁺.** The dashed line represents the experimental $^{DT}CCS_{He}$. The conformers highlighted with dark blue have been selected to be reoptimized in a larger basis set.

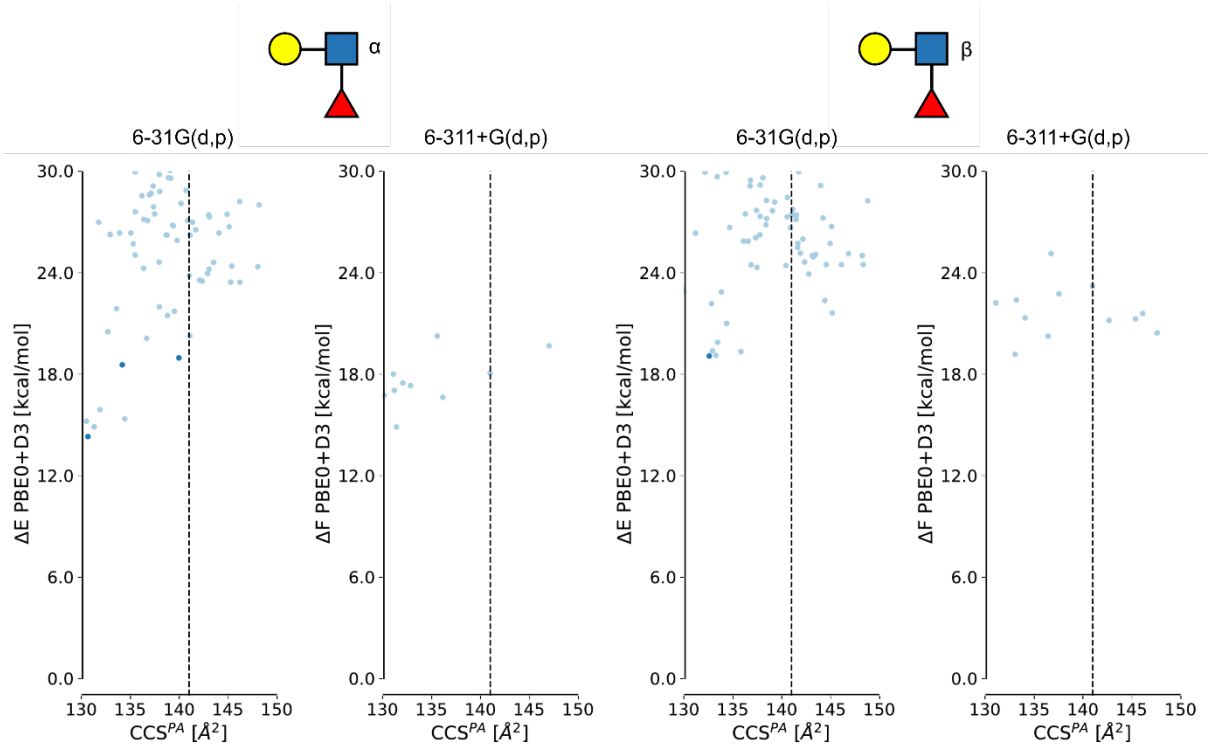

Figure S14: The CCS^{PA} vs. relative energy (ΔE, in a small 6-31G(d,p) basis set), or free-energy (ΔF, in a larger 6-311+G(d,p) basis set, evaluated at 300 K) of two anomers of the protonated **Galβ(1→4)[Fucβ(1→2)]GlcNAcα/β** and trans amide bond orientation. The glycan is shown above using the SNFG notation. The y-axis shows the (free-)energy relatively to the lowest (free-)energy conformer of the **[α-t-α16+H]⁺.** The dashed line represents the experimental $^{DT}CCS_{He}$. The conformers highlighted with dark blue have been selected to be reoptimized in a larger basis set.

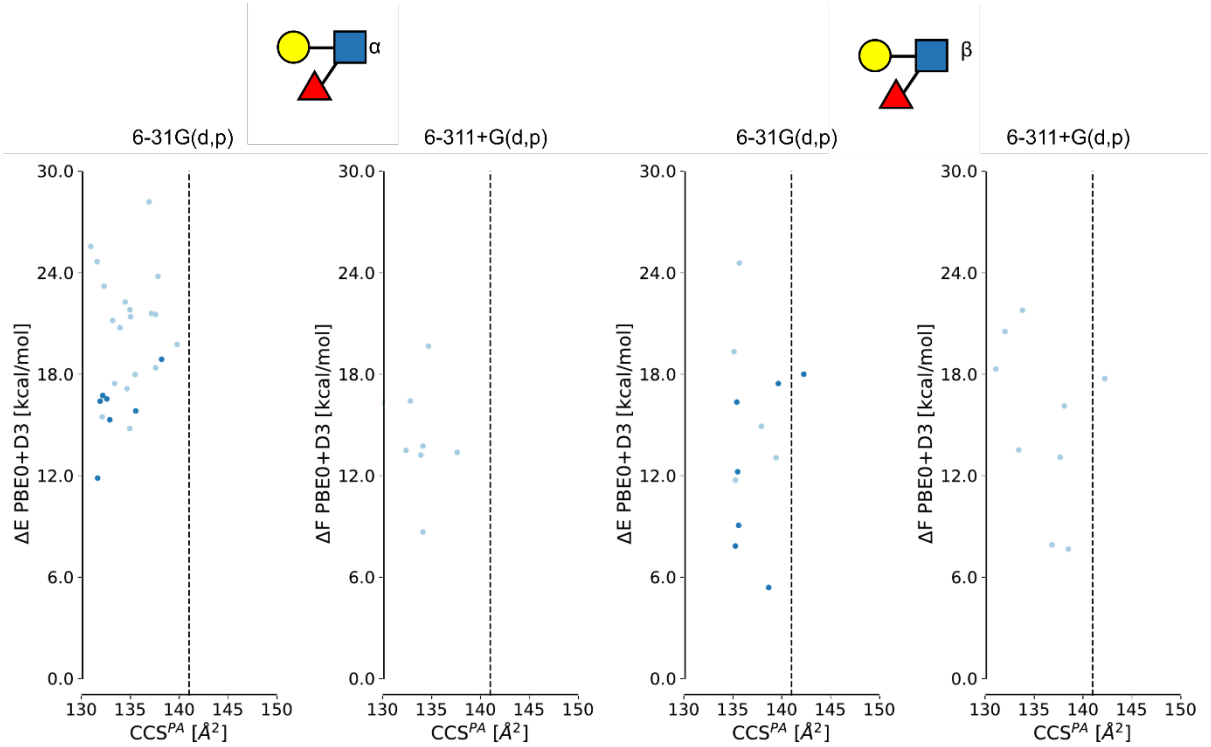

Figure S15: The CCS^{PA} vs. relative energy (ΔE, in a small 6-31G(d,p) basis set), or free-energy (ΔF, in a larger 6-311+G(d,p) basis set, evaluated at 300 K) of two anomers of the protonated **Galβ(1→4)[Fucβ(1→3)]GlcNAcα/β** and trans amide bond orientation The glycan is shown above using the SNFG notation. The y-axis shows the (free-)energy relatively to the lowest (free-)energy conformer of the **[α-t-α16+H]$^+$.** The dashed line represents the experimental ^{DT}CCS$_{He}$. The conformers highlighted with dark blue have been selected to be reoptimized in a larger basis set.

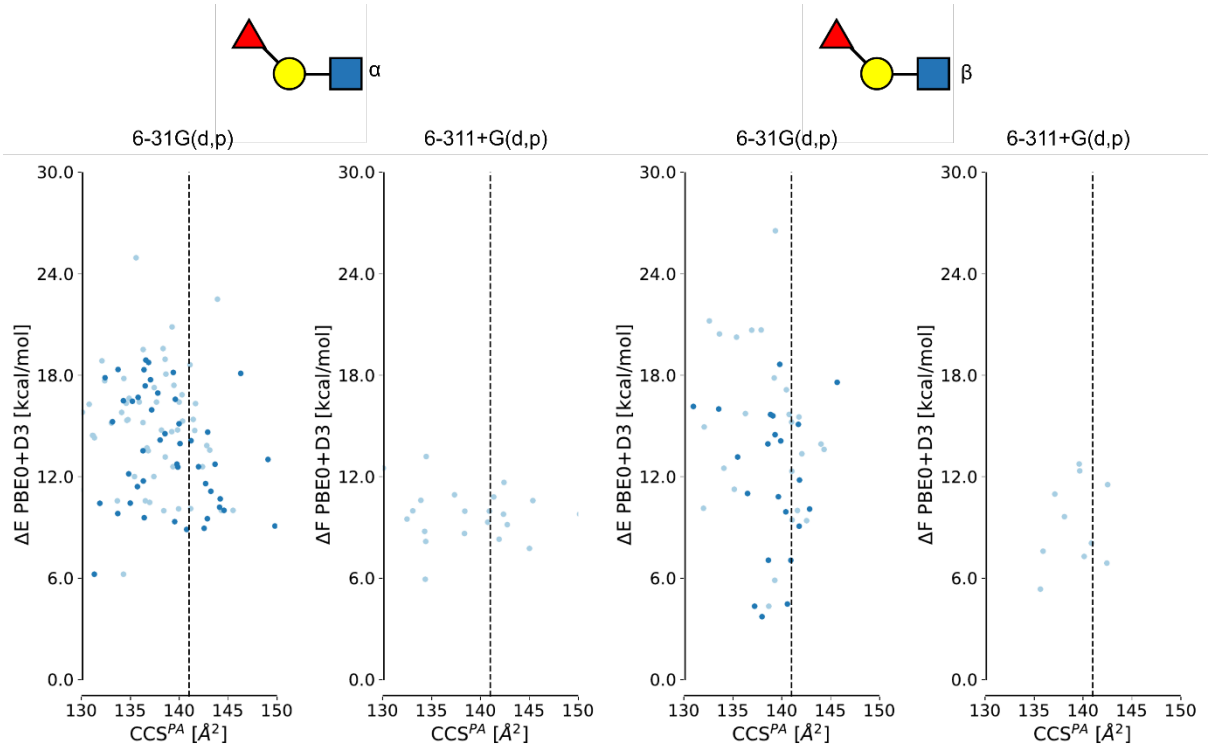

Figure S16: The CCS^{PA} vs. relative energy (ΔE, in a small 6-31G(d,p) basis set), or free-energy (ΔF, in a larger 6-311+G(d,p) basis set, evaluated at 300 K) of two anomers of the protonated **Galβ(1→4)[Fucβ(1→6)]GlcNAcα/β** and trans amide bond orientation. The glycan is shown above using the SNFG notation. The y-axis shows the (free-)energy relatively to the lowest (free-)energy conformer of the **[α-t-α16+H]$^+$.** The dashed line represents the experimental ^{DT}CCS$_{He}$. The conformers highlighted with dark blue have been selected to be reoptimized in a larger basis set.

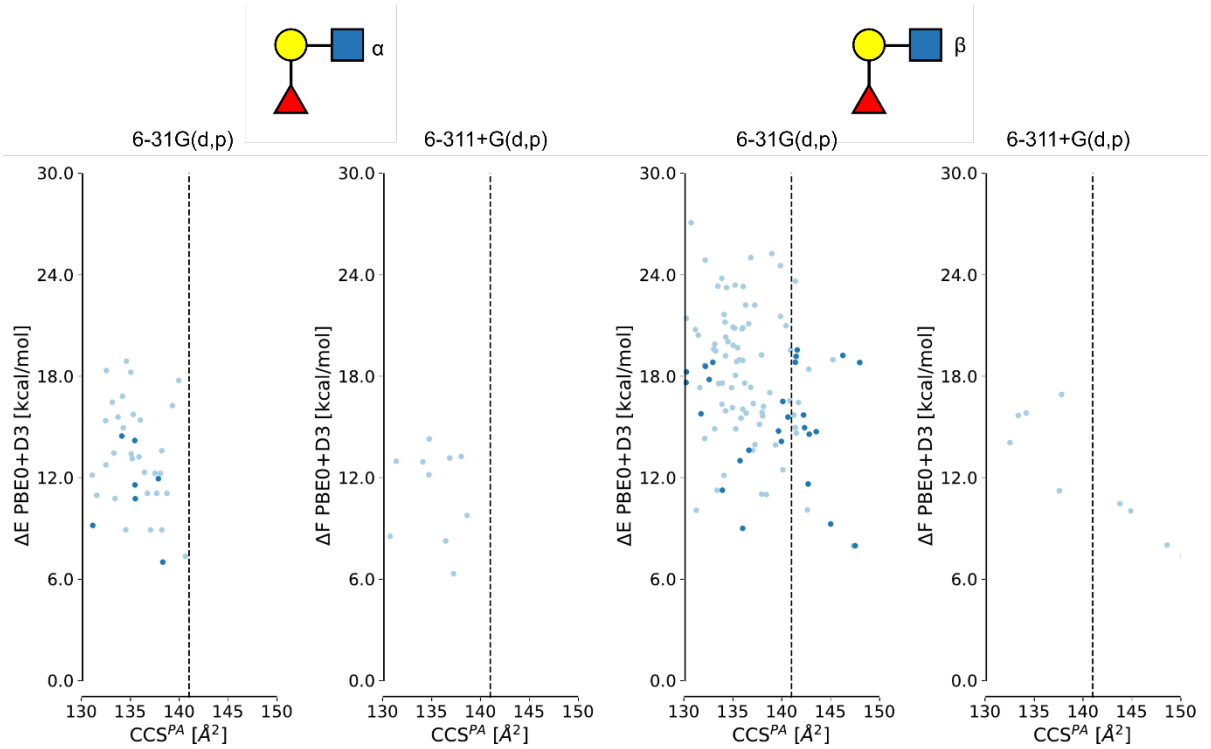

Figure S17: The CCS^{PA} vs. relative energy (ΔE, in a small 6-31G(d,p) basis set), or free-energy (ΔF, in a larger 6-311+G(d,p) basis set, evaluated at 300 K) of two anomers of the protonated **Fucβ(1→2)Galβ(1→4)GlcNAcα/β** and trans amide bond orientation. The glycan is shown above using the SNFG notation. The y-axis shows the (free-)energy relatively to the lowest (free-)energy conformer of the **[α-t-α16+H]⁺.** The dashed line represents the experimental $^{DT}CCS_{He}$. The conformers highlighted with dark blue have been selected to be reoptimized in a larger basis set.

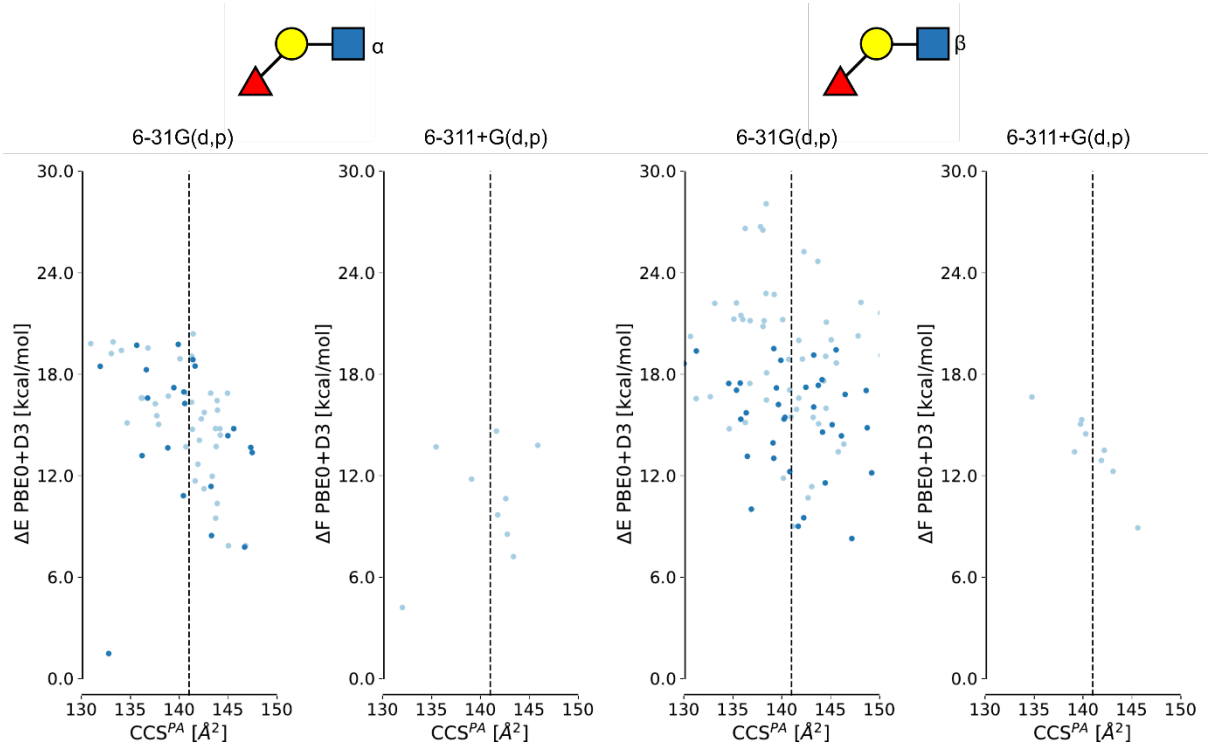

Figure S18: The CCS^{PA} vs. relative energy (ΔE, in a small 6-31G(d,p) basis set), or free-energy (ΔF, in a larger 6-311+G(d,p) basis set, evaluated at 300 K) of two anomers of the protonated **Fucβ(1→3)Galβ(1→4)GlcNAcα/β** and trans amide bond orientation. The glycan is shown above using the SNFG notation. The y-axis shows the (free-)energy relatively to the lowest (free-)energy conformer of the **[α-t-α16+H]⁺.** The dashed line represents the experimental $^{DT}CCS_{He}$. The conformers highlighted with dark blue have been selected to be reoptimized in a larger basis set.

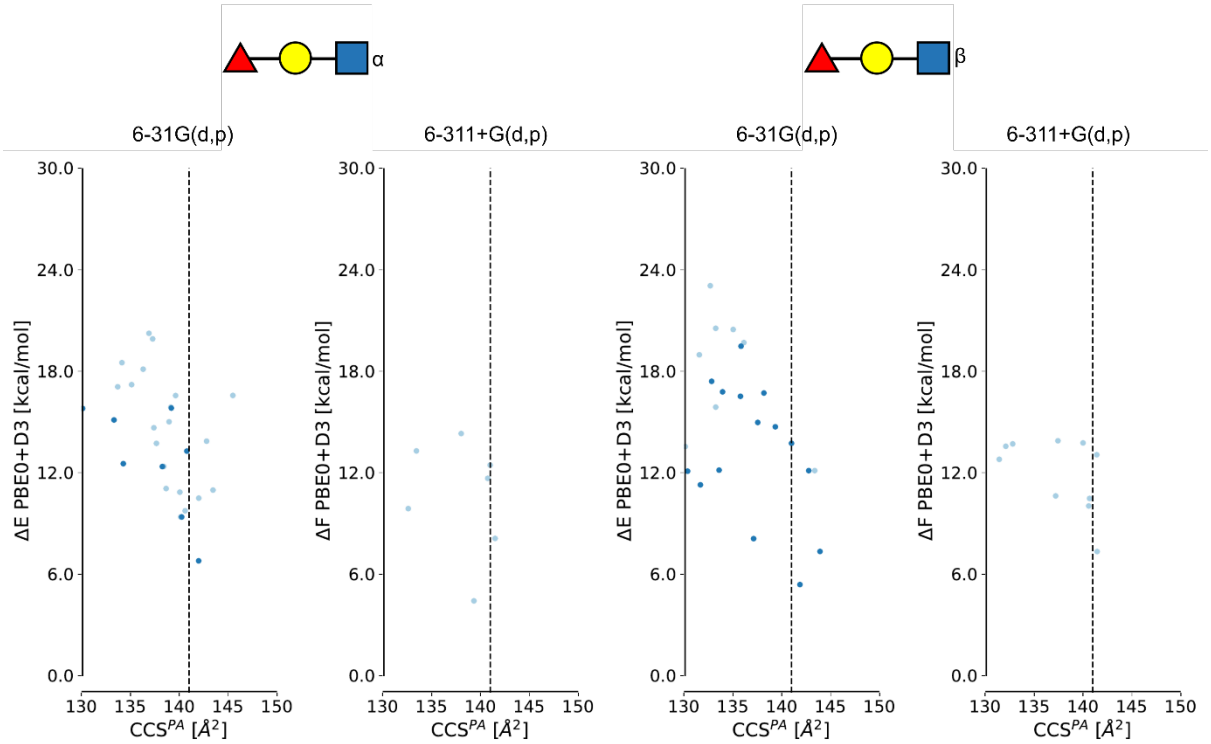

Figure S19: The CCS^{PA} vs. relative energy (ΔE, in a small 6-31G(d,p) basis set), or free-energy (ΔF, in a larger 6-311+G(d,p) basis set, evaluated at 300 K) of two anomers of the protonated **Fucβ(1→4)Galβ(1→4)GlcNAcα/β** and trans amide bond orientation. The glycan is shown above using the SNFG notation. The y-axis shows the (free-)energy relatively to the lowest (free-)energy conformer of the **[α-t-α16+H]⁺.** The dashed line represents the experimental $^{DT}CCS_{He}$. The conformers highlighted with dark blue have been selected to be reoptimized in a larger basis set.

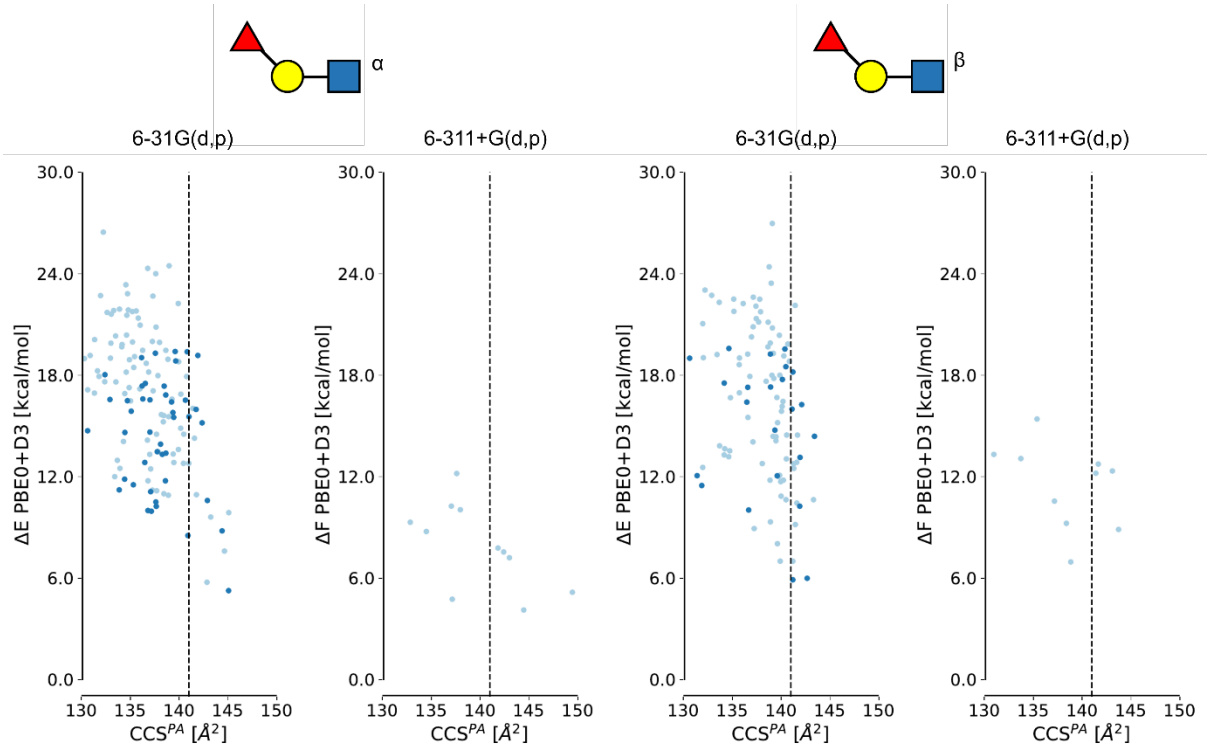

Figure S20: The CCS^{PA} vs. relative energy (ΔE, in a small 6-31G(d,p) basis set), or free-energy (ΔF, in a larger 6-311+G(d,p) basis set, evaluated at 300 K) of two anomers of the protonated **Fucβ(1→6)Galβ(1→4)GlcNAcα/β** and trans amide bond orientation. The glycan is shown above using the SNFG notation. The y-axis shows the (free-)energy relatively to the lowest (free-)energy conformer of the **[α-t-α16+H]⁺.** The dashed line represents the experimental $^{DT}CCS_{He}$. The conformers highlighted with dark blue have been selected to be reoptimized in a larger basis set.

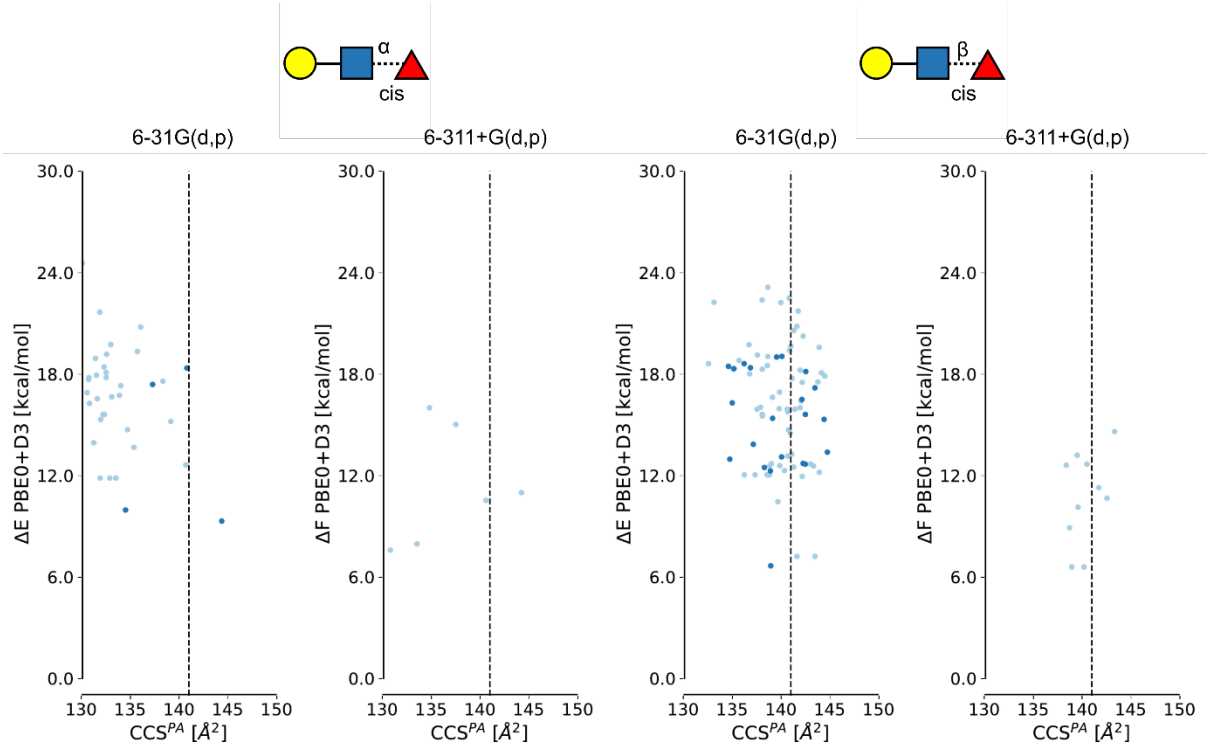

Figure S21: The CCS^{PA} vs. relative energy (ΔE, in a small 6-31G(d,p) basis set), or free-energy (ΔF, in a larger 6-311+G(d,p) basis set, evaluated at 300 K) of two anomers of the protonated **Galβ(1→4)GlcNAcα/β(1↔1)Fucα** and cis amide bond orientation. The glycan is shown above using the SNFG notation. The y-axis shows the (free-)energy relatively to the lowest (free-)energy conformer of the **[α-t-α16+H]⁺.** The dashed line represents the experimental $^{DT}CCS_{He}$. The conformers highlighted with dark blue have been selected to be reoptimized in a larger basis set.

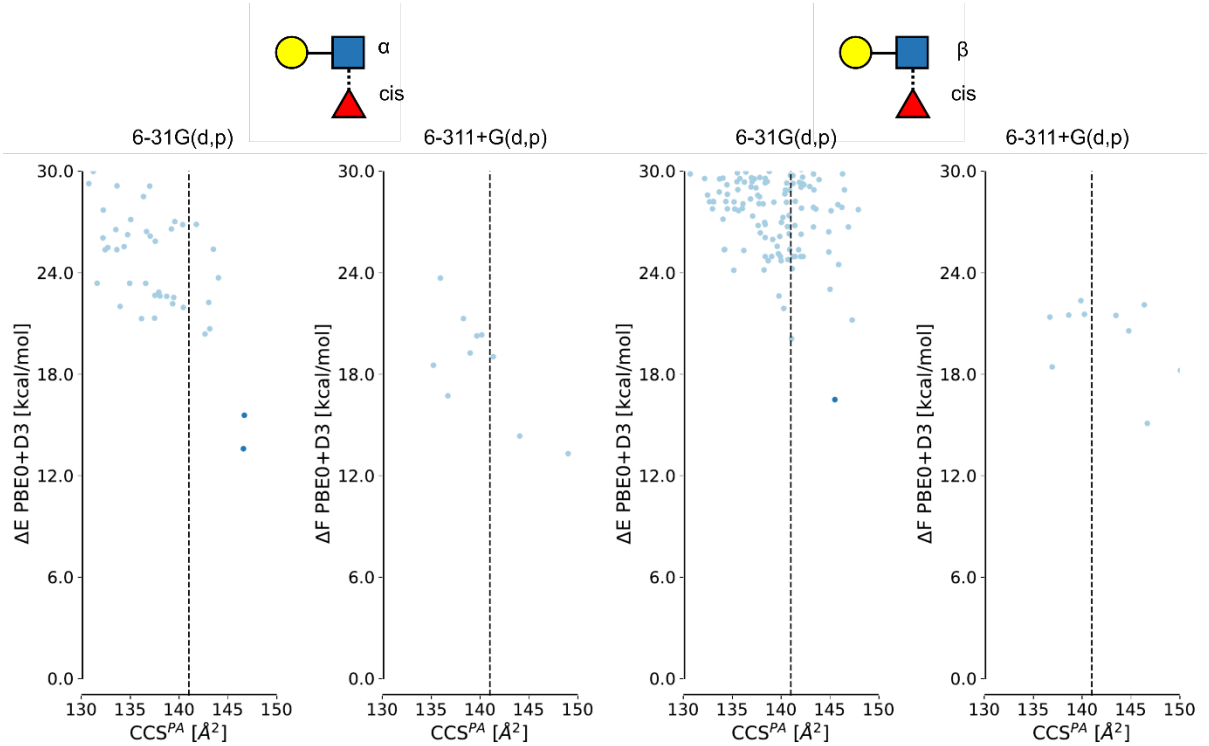

Figure S22: The CCS^{PA} vs. relative energy (ΔE, in a small 6-31G(d,p) basis set), or free-energy (ΔF, in a larger 6-311+G(d,p) basis set, evaluated at 300 K) of two anomers of the protonated **Galβ(1→4)[Fucα(1→2)]GlcNAcα/β** and cis amide bond orientation. The glycan is shown above using the SNFG notation. The y-axis shows the (free-)energy relatively to the lowest (free-)energy conformer of the **[α-t-α16+H]⁺.** The dashed line represents the experimental $^{DT}CCS_{He}$. The conformers highlighted with dark blue have been selected to be reoptimized in a larger basis set.

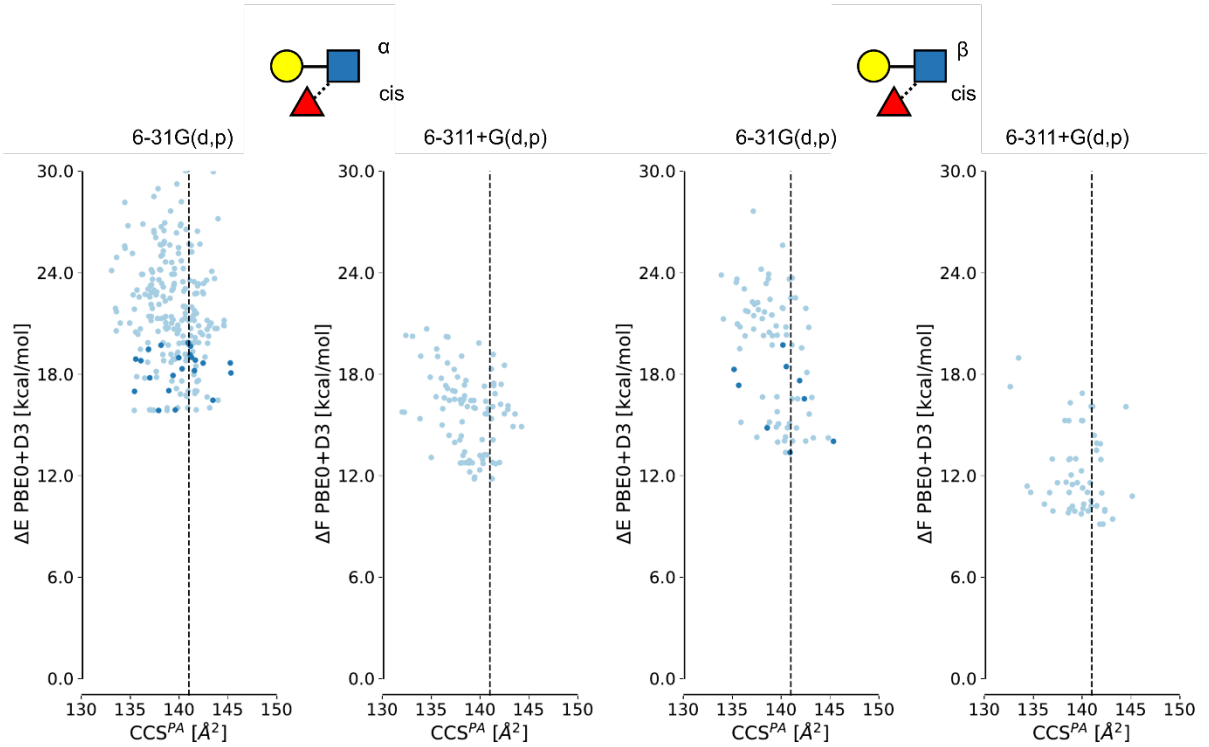

Figure S23: The CCS^{PA} vs. relative energy (ΔE, in a small 6-31G(d,p) basis set), or free-energy (ΔF, in a larger 6-311+G(d,p) basis set, evaluated at 300 K) of two anomers of the protonated **Galβ(1→4)[Fucα(1→3)]GlcNAcα/β** and cis amide bond orientation. The glycan is shown above using the SNFG notation. The y-axis shows the (free-)energy relatively to the lowest (free-)energy conformer of the **[α-t-α16+H]⁺.** The dashed line represents the experimental $^{DT}CCS_{He}$. The conformers highlighted with dark blue have been selected to be reoptimized in a larger basis set.

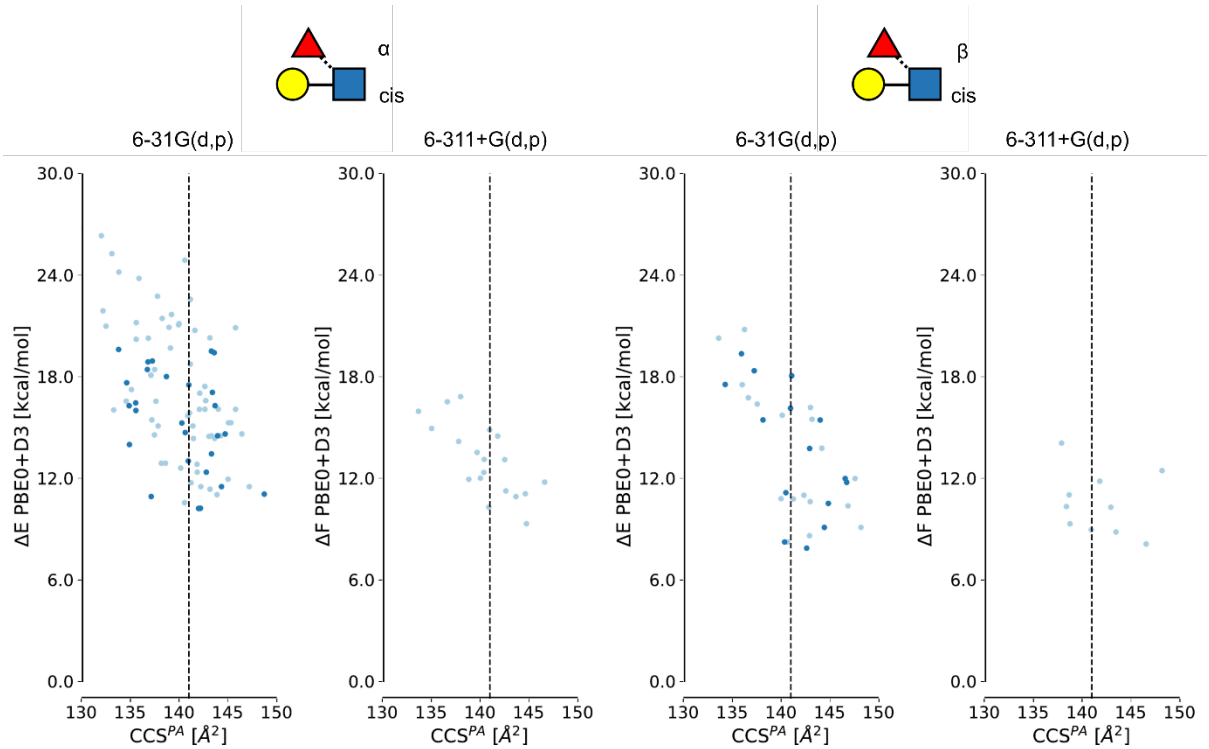

Figure S24: The CCS^{PA} vs. relative energy (ΔE, in a small 6-31G(d,p) basis set), or free-energy (ΔF, in a larger 6-311+G(d,p) basis set, evaluated at 300 K) of two anomers of the protonated **Galβ(1→4)[Fucα(1→6)]GlcNAcα/β** and cis amide bond orientation. The glycan is shown above using the SNFG notation. The y-axis shows the (free-)energy relatively to the lowest (free-)energy conformer of **[α-t-α16+H]⁺.** The dashed line represents the experimental $^{DT}CCS_{He}$. The conformers highlighted with dark blue have been selected to be reoptimized in a larger basis set.

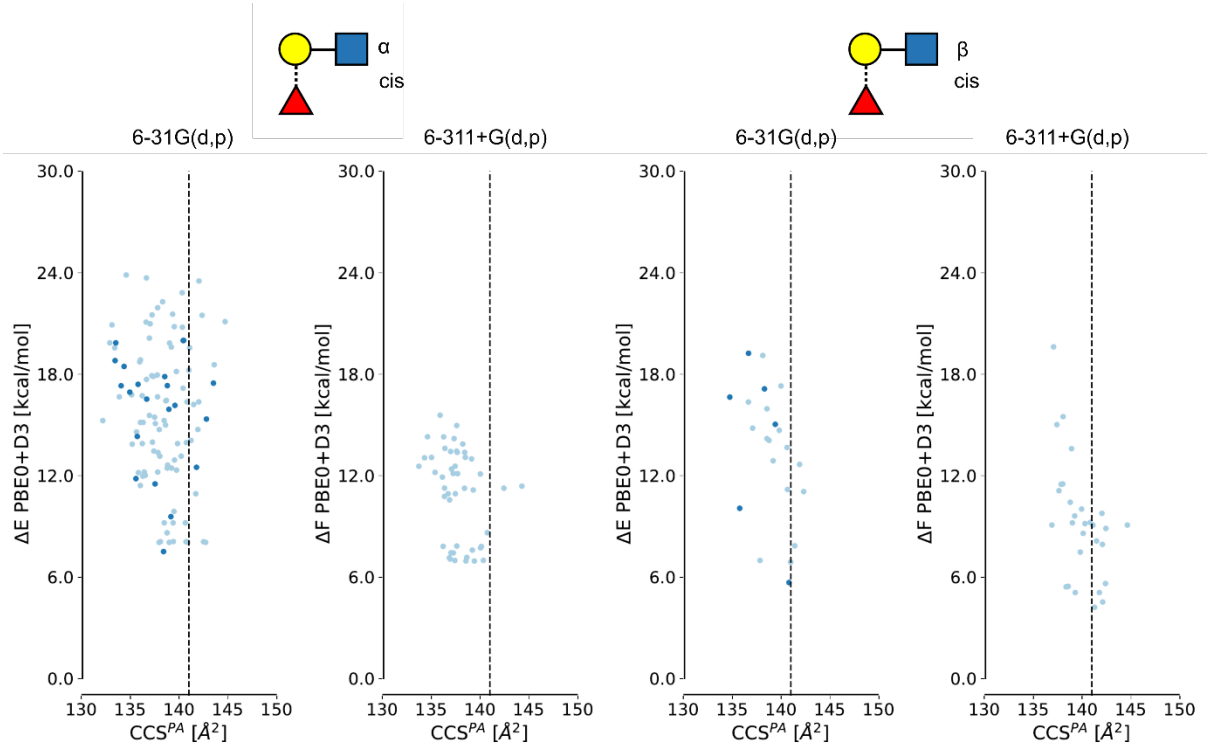

Figure S25: The CCS^{PA} vs. relative energy (ΔE, in a small 6-31G(d,p) basis set), or free-energy (ΔF, in a larger 6-311+G(d,p) basis set, evaluated at 300 K) of two anomers of the protonated **Fucα(1→2)Galβ(1→4)GlcNAcα/β** and cis amide bond orientation. The glycan is shown above using the SNFG notation. The y-axis shows the (free-)energy relatively to the lowest (free-)energy conformer of the **[α-t-α16+H]⁺.** The dashed line represents the experimental $^{DT}CCS_{He}$. The conformers highlighted with dark blue have been selected to be reoptimized in a larger basis set.

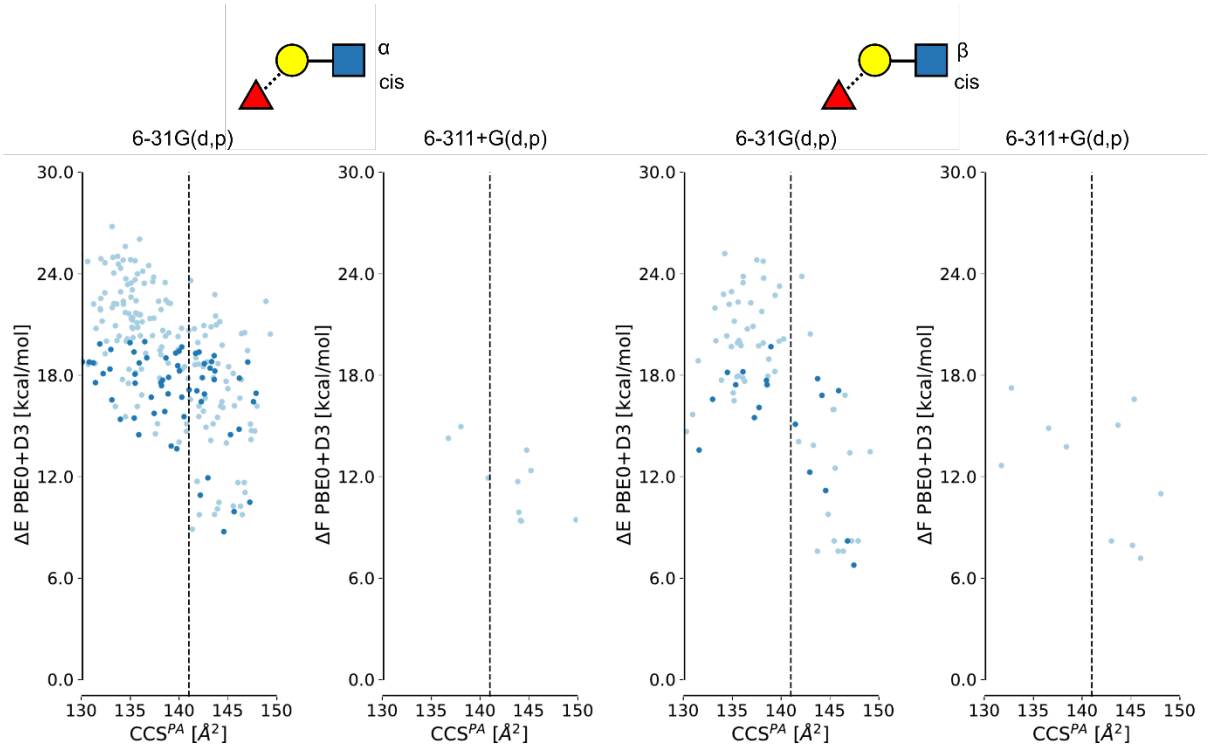

Figure S26: The CCS^{PA} vs. relative energy (ΔE, in a small 6-31G(d,p) basis set), or free-energy (ΔF, in a larger 6-311+G(d,p) basis set, evaluated at 300 K) of two anomers of the protonated **Fucα(1→3)Galβ(1→4)GlcNAcα/β** and cis amide bond orientation. The glycan is shown above using the SNFG notation. The y-axis shows the (free-)energy relatively to the lowest (free-)energy conformer of the **[α-t-α16+H]⁺.** The dashed line represents the experimental $^{DT}CCS_{He}$. The conformers highlighted with dark blue have been selected to be reoptimized in a larger basis set.

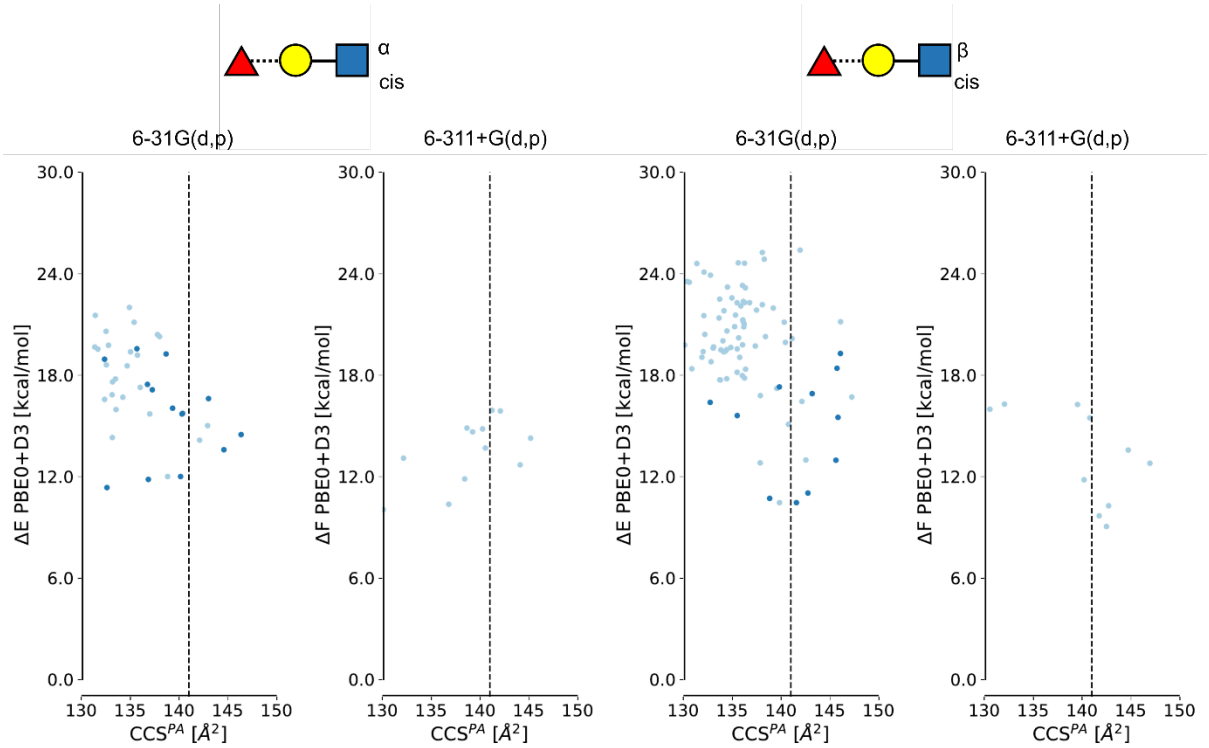

Figure S27: The CCS^{PA} vs. relative energy (ΔE, in a small 6-31G(d,p) basis set), or free-energy (ΔF, in a larger 6-311+G(d,p) basis set, evaluated at 300 K) of two anomers of the protonated **Fucα(1→4)Galβ(1→4)GlcNAcα/β** and cis amide bond orientation. The glycan is shown above using the SNFG notation. The y-axis shows the (free-)energy relatively to the lowest (free-)energy conformer of the **[α-t-α16+H]⁺.** The dashed line represents the experimental $^{DT}CCS_{He}$. The conformers highlighted with dark blue have been selected to be reoptimized in a larger basis set.

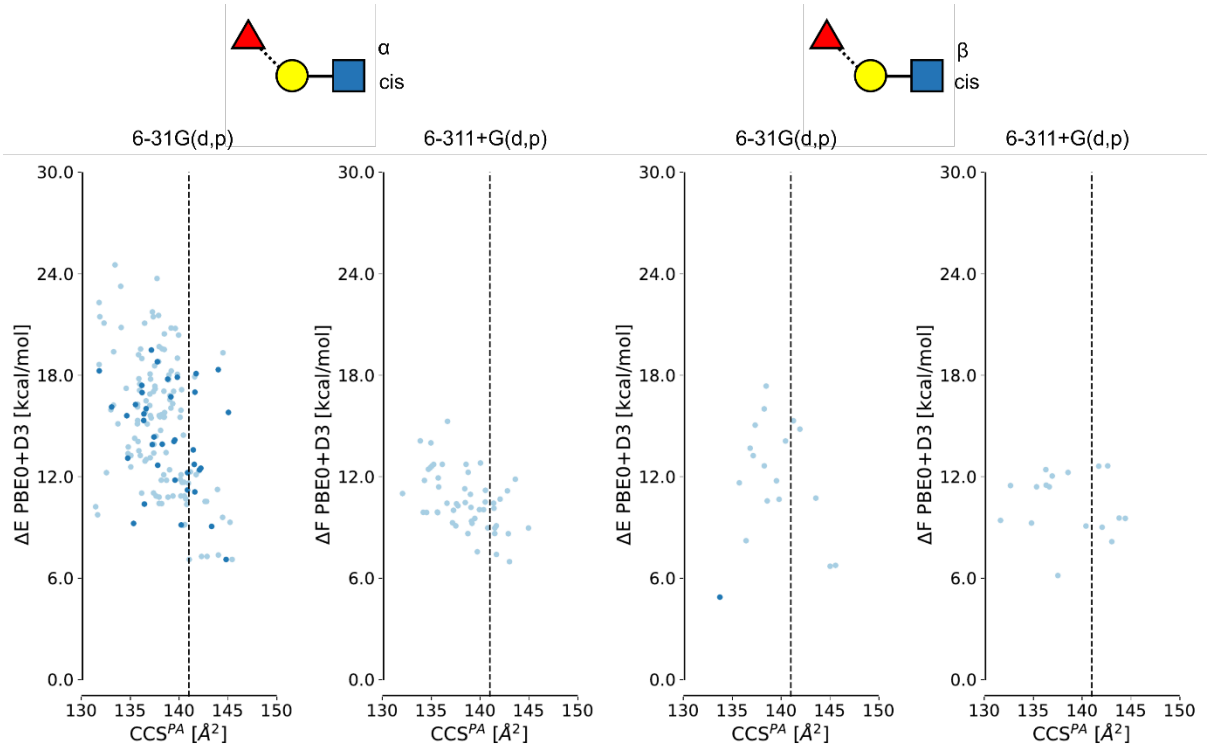

Figure S28: The CCS^{PA} vs. relative energy (ΔE, in a small 6-31G(d,p) basis set), or free-energy (ΔF, in a larger 6-311+G(d,p) basis set, evaluated at 300 K) of two anomers of the protonated **Fucα(1→6)Galβ(1→4)GlcNAcα/β** and cis amide bond orientation. The glycan is shown above using the SNFG notation. The y-axis shows the (free-)energy relatively to the lowest (free-)energy conformer of the **[α-t-α16+H]⁺.** The dashed line represents the experimental $^{DT}CCS_{He}$. The conformers highlighted with dark blue have been selected to be reoptimized in a larger basis set.

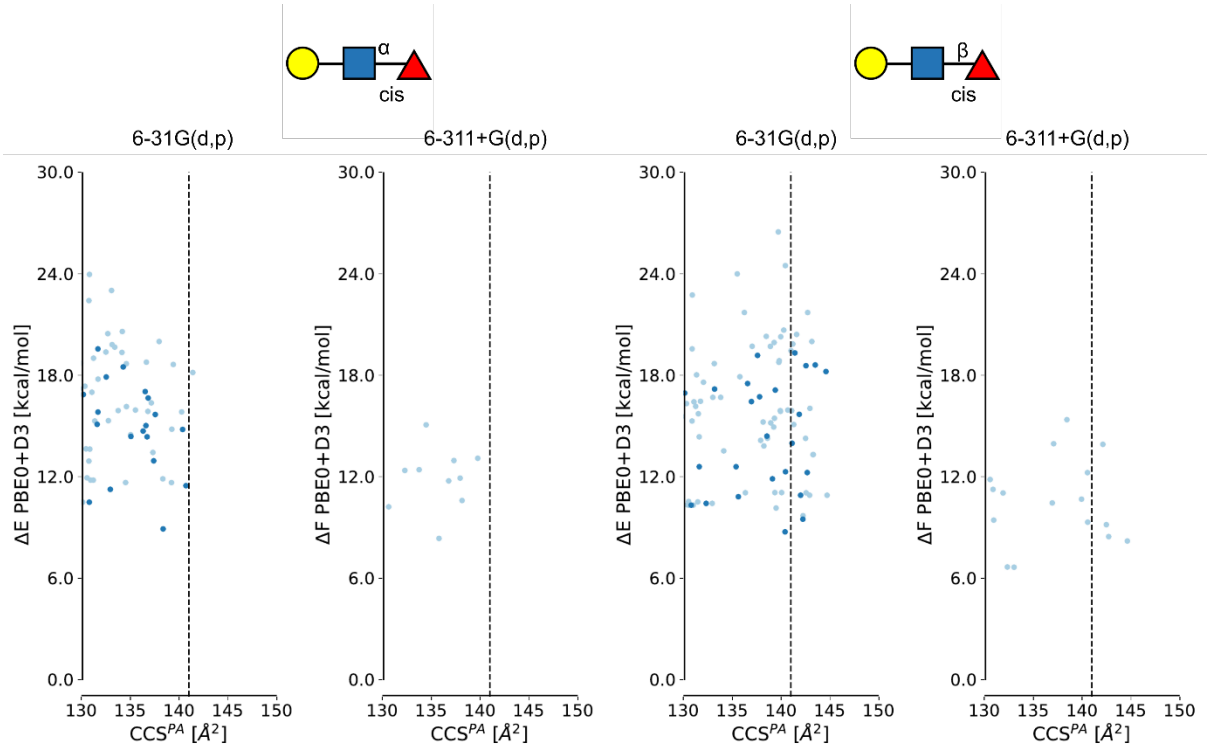

Figure S29: The CCS^{PA} vs. relative energy (ΔE, in a small 6-31G(d,p) basis set), or free-energy (ΔF, in a larger 6-311+G(d,p) basis set, evaluated at 300 K) of two anomers of the protonated **Galβ(1→4)GlcNAcα/β(1↔1)Fucβ** and cis amide bond orientation. The glycan is shown above using the SNFG notation. The y-axis shows the (free-)energy relatively to the lowest (free-)energy conformer of the **[α-t-α16+H]⁺.** The dashed line represents the experimental $^{DT}CCS_{He}$. The conformers highlighted with dark blue have been selected to be reoptimized in a larger basis set.

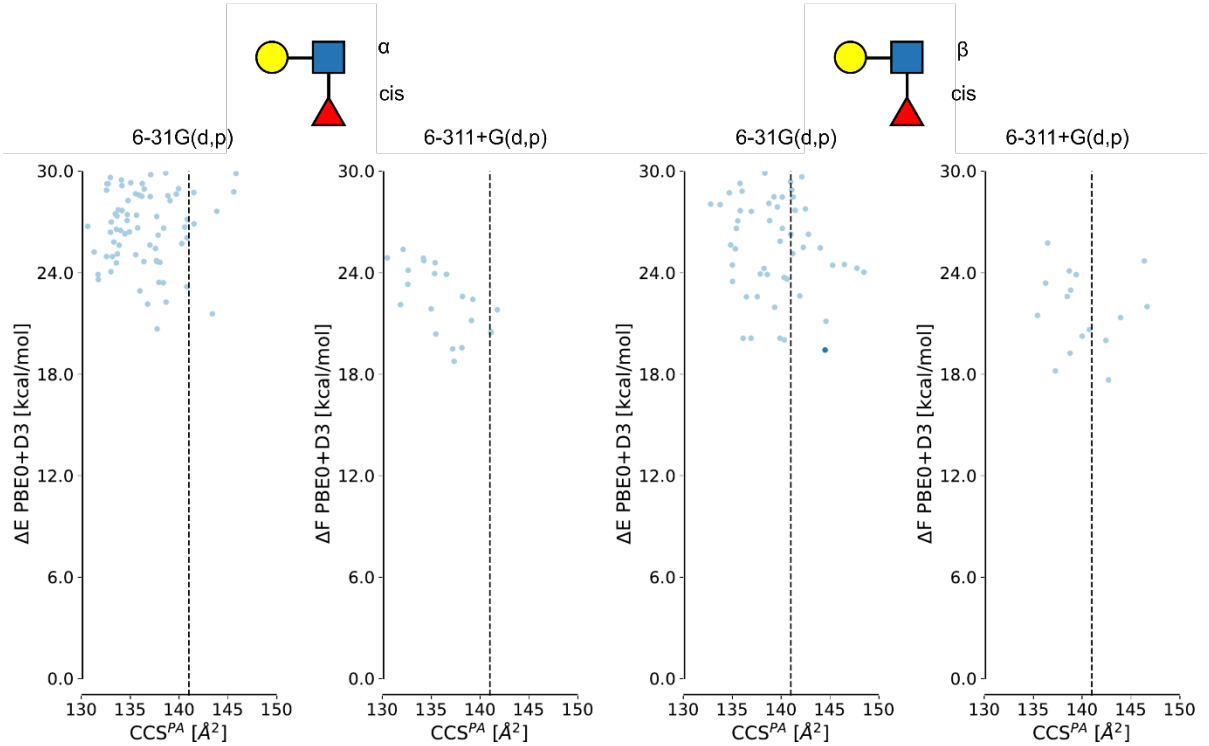

Figure S30: The CCS^{PA} vs. relative energy (ΔE, in a small 6-31G(d,p) basis set), or free-energy (ΔF, in a larger 6-311+G(d,p) basis set, evaluated at 300 K) of two anomers of the protonated **Galβ(1→4)[Fucβ(1→2)]GlcNAcα/β** and cis amide bond orientation. The glycan is shown above using the SNFG notation. The y-axis shows the (free-)energy relatively to the lowest (free-)energy conformer of **[α-t-α16+H]⁺.** The dashed line represents the experimental $^{DT}CCS_{He}$. The conformers highlighted with dark blue have been selected to be reoptimized in a larger basis set.

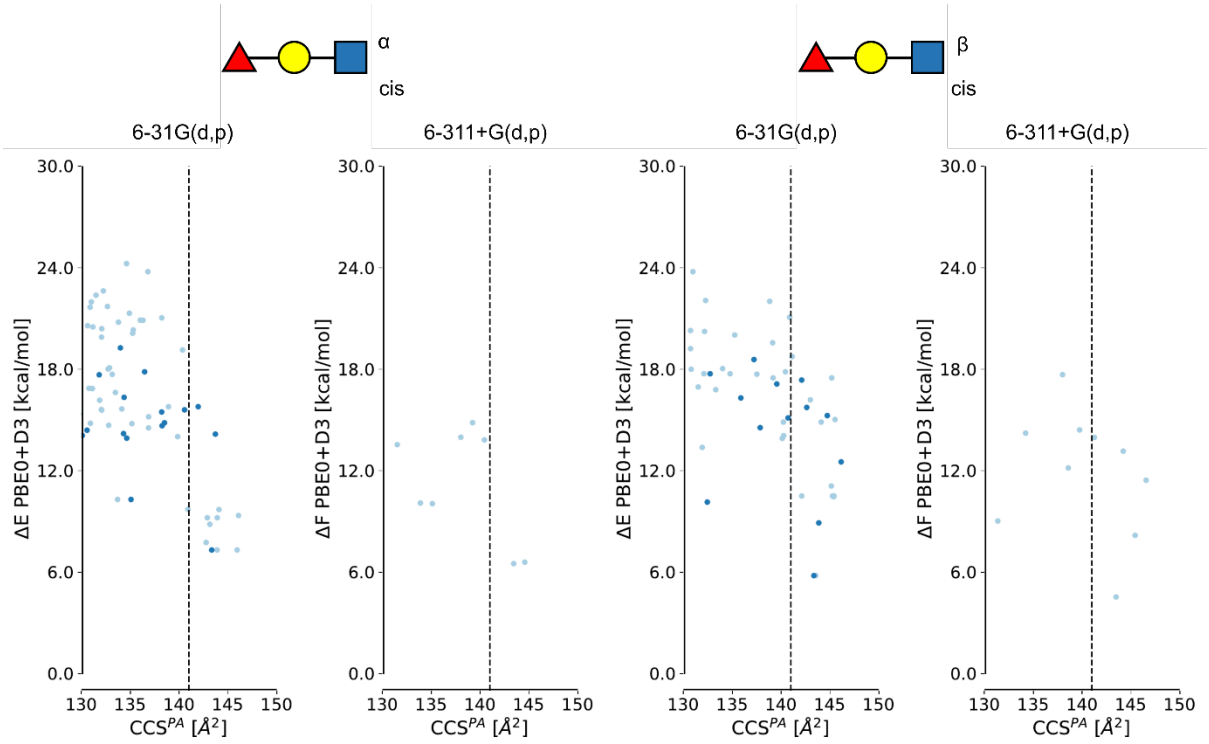

Figure S31: The CCS^{PA} vs. relative energy (ΔE, in a small 6-31G(d,p) basis set), or free-energy (ΔF, in a larger 6-311+G(d,p) basis set, evaluated at 300 K) of two anomers of the protonated **Galβ(1→4)[Fucβ(1→3)]GlcNAcα/β** and cis amide bond orientation. The glycan is shown above using the SNFG notation. The y-axis shows the (free-)energy relatively to the lowest (free-)energy conformer of **[α-t-α16+H]⁺.** The dashed line represents the experimental $^{DT}CCS_{He}$. The conformers highlighted with dark blue have been selected to be reoptimized in a larger basis set.

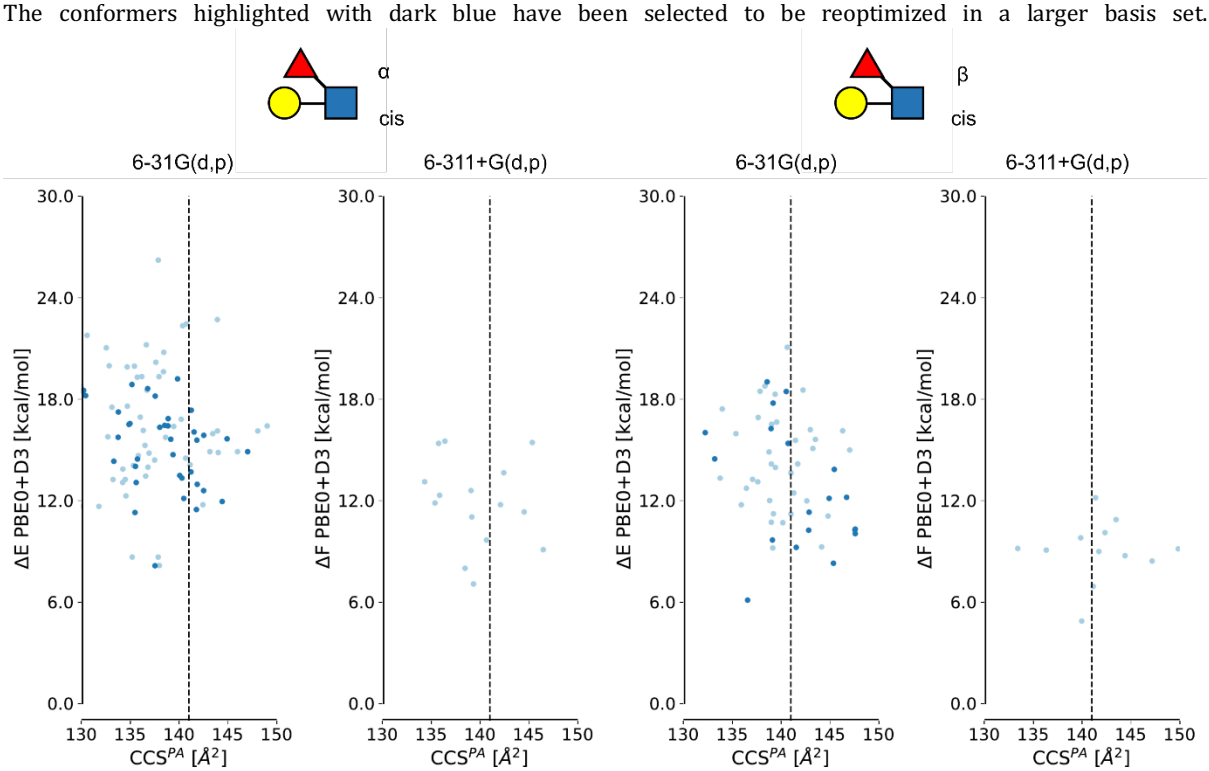

Figure S32: The CCS^{PA} vs. relative energy (ΔE, in a small 6-31G(d,p) basis set), or free-energy (ΔF, in a larger 6-311+G(d,p) basis set, evaluated at 300 K) of two anomers of the protonated **Galβ(1→4)[Fucβ(1→6)]GlcNAcα/β** and cis amide bond orientation. The glycan is shown above using the SNFG notation. The y-axis shows the (free-)energy relatively to the lowest (free-)energy conformer of **[α-t-α16+H]⁺.** The dashed line represents the experimental $^{DT}CCS_{He}$. The conformers highlighted with dark blue have been selected to be reoptimized in a larger basis set.

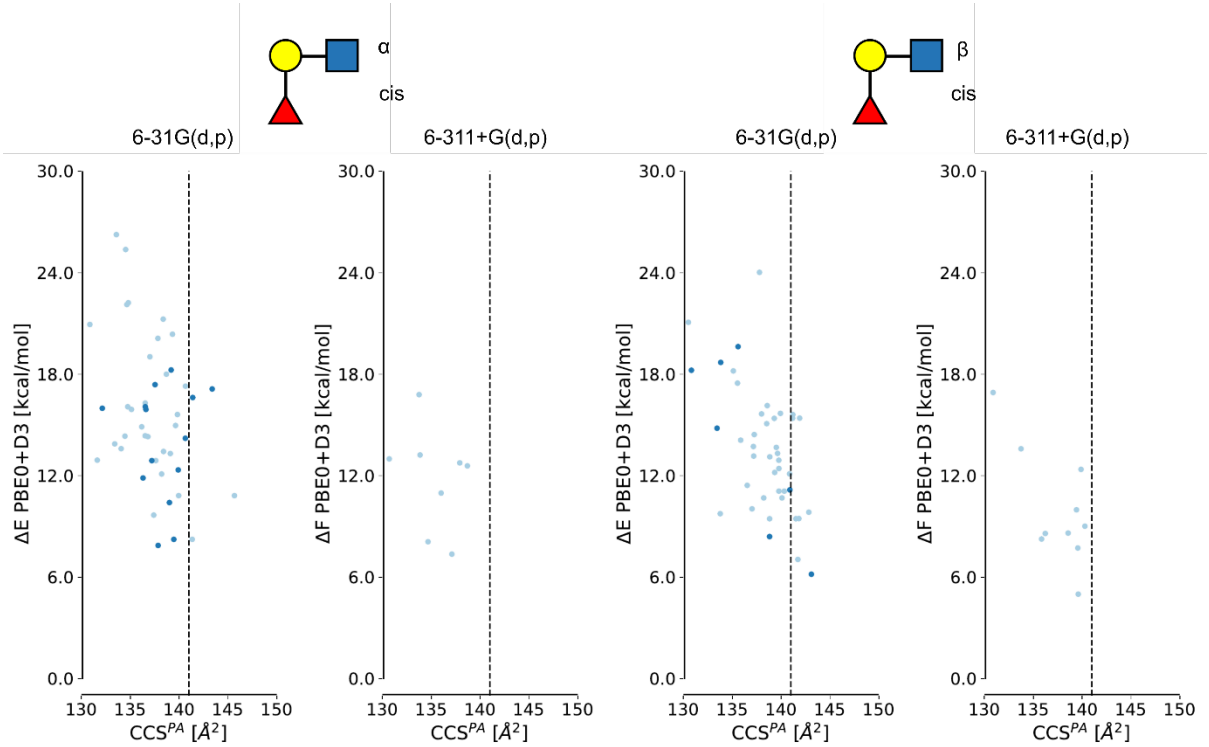

Figure S33: The CCS^{PA} vs. relative energy (ΔE, in a small 6-31G(d,p) basis set), or free-energy (ΔF, in a larger 6-311+G(d,p) basis set, evaluated at 300 K) of two anomers of the protonated **Fucβ(1→2)Galβ(1→4)GlcNAcα/β** and cis amide bond orientation. The glycan is shown above using the SNFG notation. The y-axis shows the (free-)energy relatively to the lowest (free-)energy conformer of the **[α-t-α16+H]⁺.** The dashed line represents the experimental $^{DT}CCS_{He}$. The conformers highlighted with dark blue have been selected to be reoptimized in a larger basis set.

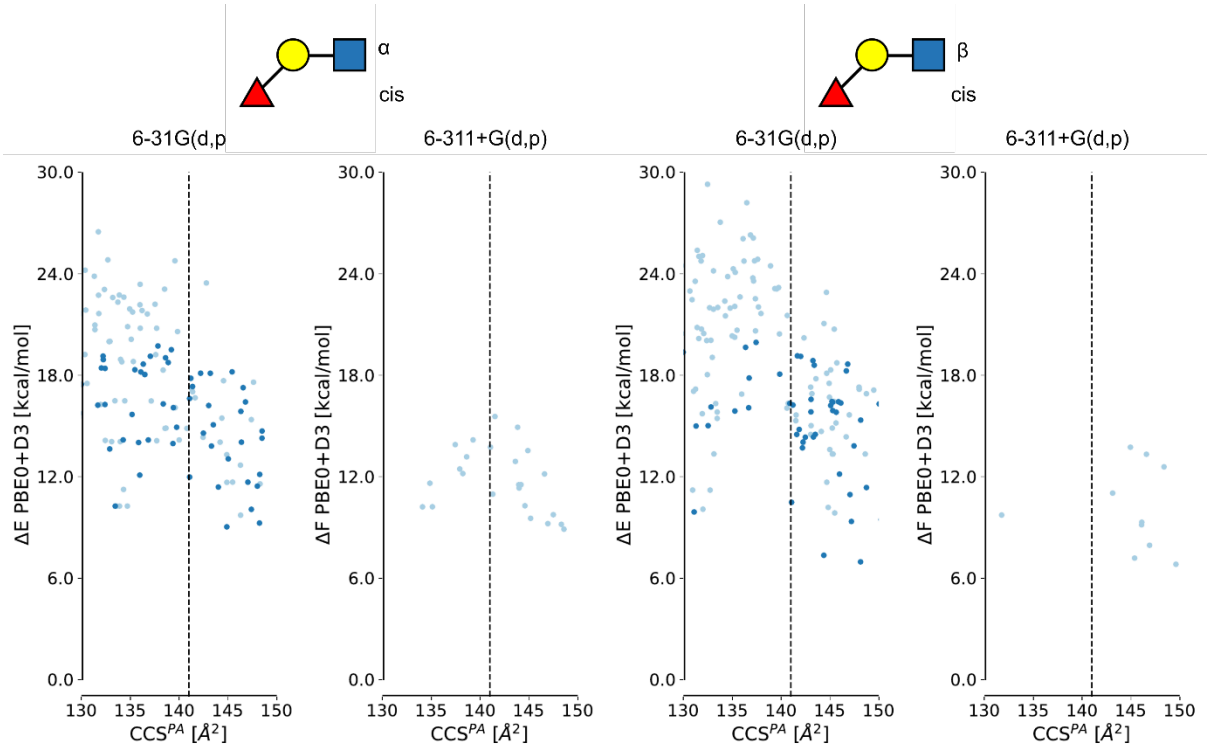

Figure S34: The CCS^{PA} vs. relative energy (ΔE, in a small 6-31G(d,p) basis set), or free-energy (ΔF, in a larger 6-311+G(d,p) basis set, evaluated at 300 K) of two anomers of the protonated **Fucβ(1→3)Galβ(1→4)GlcNAcα/β** and cis amide bond orientation. The glycan is shown above using the SNFG notation. The y-axis shows the (free-)energy relatively to the lowest (free-)energy conformer of the **[α-t-α16+H]⁺.** The dashed line represents the experimental $^{DT}CCS_{He}$. The conformers highlighted with dark blue have been selected to be reoptimized in a larger basis set.

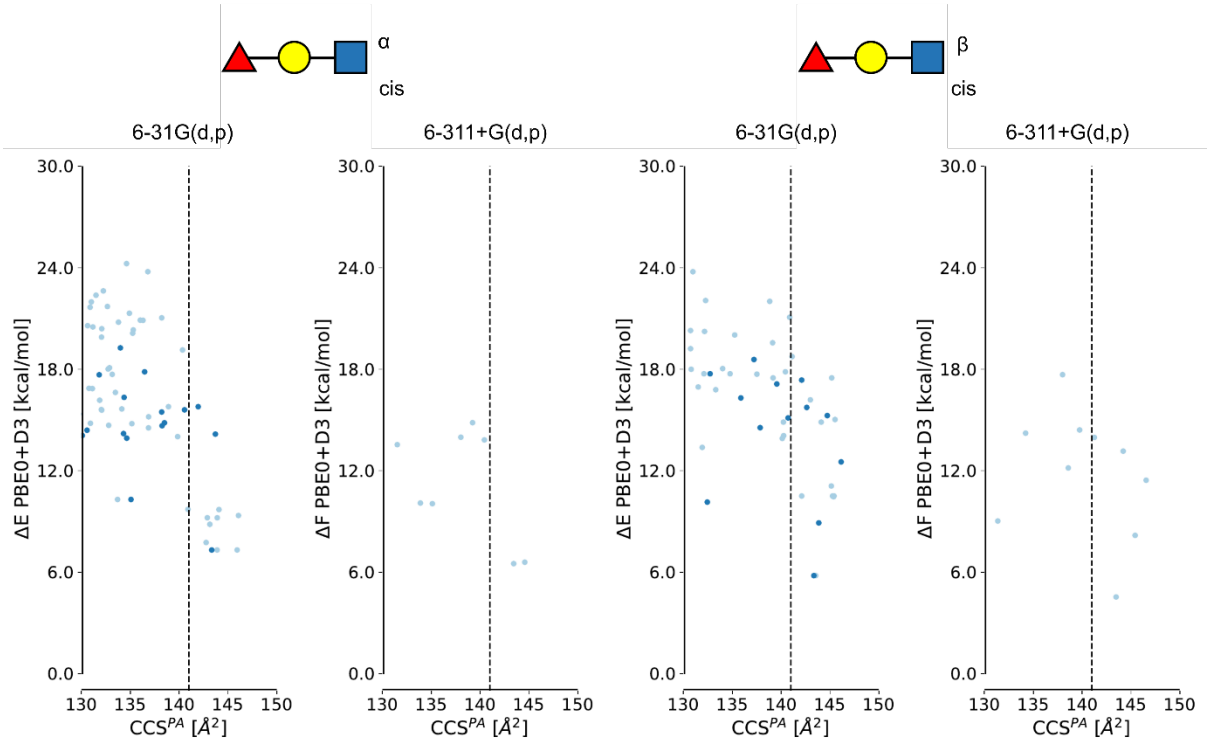

Figure S35: The CCS^{PA} vs. relative energy (ΔE, in a small 6-31G(d,p) basis set), or free-energy (ΔF, in a larger 6-311+G(d,p) basis set, evaluated at 300 K) of two anomers of the protonated **Fucβ(1→4)Galβ(1→4)GlcNAcα/β** and cis amide bond orientation. The glycan is shown above using the SNFG notation. The y-axis shows the (free-)energy relatively to the lowest (free-)energy conformer of the **[α-t-α16+H]⁺.** The dashed line represents the experimental $^{DT}CCS_{He}$. The conformers highlighted with dark blue have been selected to be reoptimized in a larger basis set.

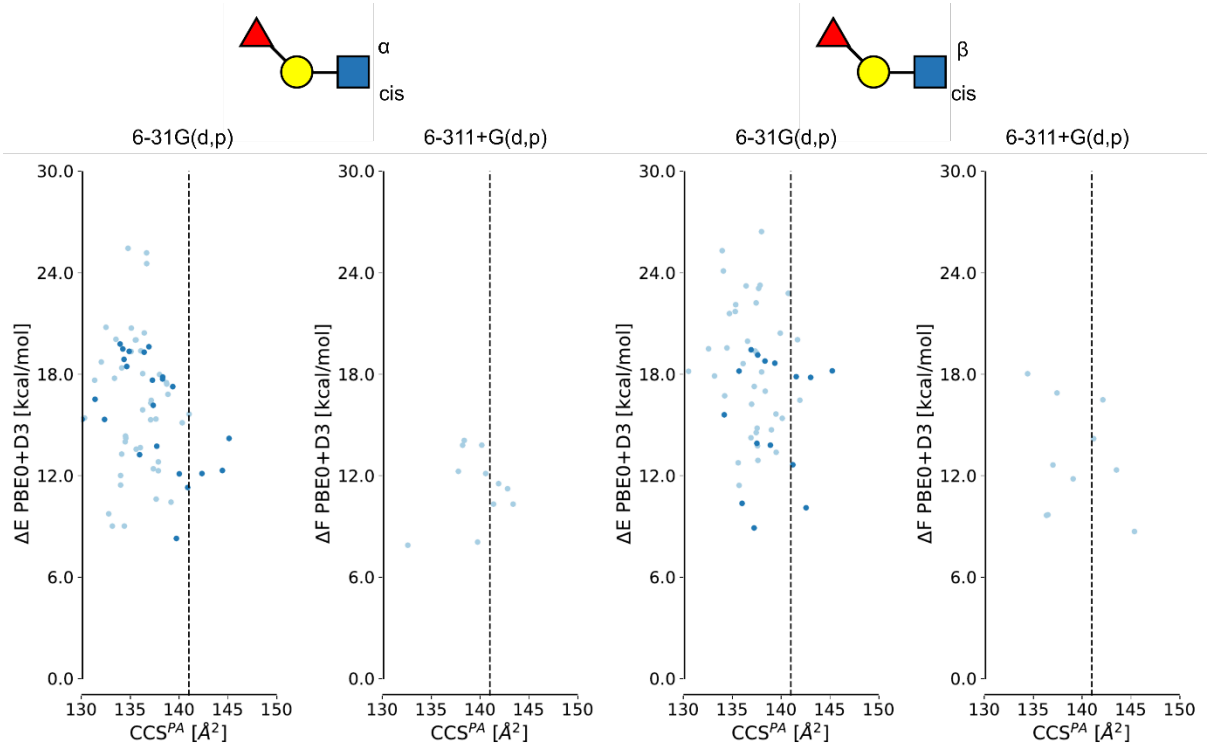

Figure S36: The CCS^{PA} vs. relative energy (ΔE, in a small 6-31G(d,p) basis set), or free-energy (ΔF, in a larger 6-311+G(d,p) basis set, evaluated at 300 K) of two anomers of the protonated **Fucβ(1→6)Galβ(1→4)GlcNAcα/β** and cis amide bond orientation. The glycan is shown above using the SNFG notation. The y-axis shows the (free-)energy relatively to the lowest (free-)energy conformer of the **[α-t-α16+H]⁺.** The dashed line represents the experimental $^{DT}CCS_{He}$. The conformers highlighted with dark blue have been selected to be reoptimized in a larger basis set.

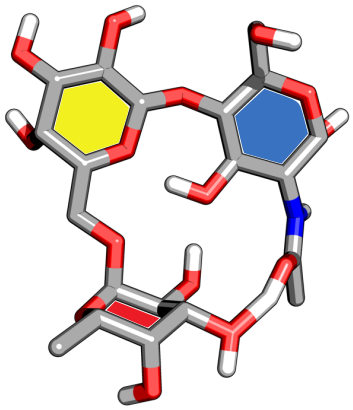

Figure S37: Structure of the most stable conformer of **[α-t-α16+H]⁺.**

Table S2: XYZ-coordinates of the most stable conformer of **[α-t-α16+H]⁺.**

C	2.308714	-3.815044	0.072271
O	3.293236	-3.159541	0.801517
C	3.649276	-1.850123	0.351808
C	2.425125	-0.940149	0.312734
C	1.281813	-1.578800	-0.467809
C	1.025584	-2.991768	0.051518
N	0.037629	-3.650234	-0.793378
C	-1.251729	-3.672293	-0.569137
O	-1.663098	-3.258347	0.571896
H	-2.635034	-2.948389	0.592069
C	-2.192256	-4.162491	-1.602621
H	-2.739295	-3.285621	-1.966876
H	-1.674788	-4.635080	-2.437046
H	-2.899342	-4.866418	-1.159374
H	0.385002	-4.008484	-1.674827
H	0.623143	-2.931628	1.063278
O	0.074228	-0.873961	-0.322914
H	0.253220	0.088669	-0.423351
H	1.582270	-1.626834	-1.524182
H	2.100565	-0.735248	1.341440
O	2.845969	0.267082	-0.312351
C	2.276420	1.442969	0.141447
C	3.126814	2.618115	-0.304336
C	2.462241	3.904822	0.161473
O	3.146345	5.034147	-0.319130
H	4.082410	4.918960	-0.126493
C	1.032635	4.004701	-0.361246
C	0.268787	2.729066	-0.033691
C	-1.073539	2.678486	-0.723715
H	-1.683642	3.528165	-0.396289
H	-0.933394	2.738363	-1.807722
O	-1.690299	1.448388	-0.375305
C	-2.962378	1.258211	-0.924003
O	-3.950213	2.002591	-0.256456
C	-4.041053	1.715684	1.143731
C	-5.041467	2.676711	1.739385
H	-6.032689	2.544967	1.300376
H	-5.122116	2.517841	2.817316
H	-4.721536	3.704476	1.560358
C	-4.404568	0.248642	1.339953
C	-3.392776	-0.637125	0.622954
C	-3.272005	-0.237490	-0.843640

O	-2.354872	-1.023386	-1.551989
H	-1.464198	-0.891860	-1.173528
H	-4.241441	-0.386326	-1.330735
H	-2.412939	-0.563640	1.102721
O	-3.795466	-2.004485	0.748026
H	-4.754393	-2.046194	0.627602
O	-5.700477	-0.082163	0.868432
H	-5.915445	0.495236	0.128197
H	-4.397533	0.012177	2.408703
H	-3.055938	1.871296	1.601691
H	-2.988327	1.598574	-1.964903
H	0.124306	2.675654	1.056331
O	0.994005	1.574680	-0.454917
H	0.536690	4.842104	0.152550
O	1.020304	4.197472	-1.751839
H	1.669849	4.883624	-1.943981
H	2.444147	3.903122	1.262827
O	4.414012	2.599017	0.265414
H	4.947611	1.949620	-0.197580
H	3.165473	2.606251	-1.400478
H	2.173932	1.422909	1.239889
C	4.688690	-1.348319	1.336780
O	4.166072	-1.224300	2.636405
H	4.030986	-2.107189	2.989390
H	5.555715	-2.019020	1.308904
H	5.016847	-0.353518	1.030807
H	4.085493	-1.904303	-0.653565
O	2.652243	-4.032258	-1.270595
H	3.379444	-4.659632	-1.318851
H	2.149674	-4.763305	0.596307

Additional References

1. "Additive CHARMM36 Force Field for Nonstandard Amino Acids", Anastasia Croitoru, Sang-Jun Park, Anmol Kumar, Jumin Lee, Wonpil Im, Alexander D. MacKerell Jr., and Alexey Aleksandrov, *Journal of Chemical Theory and Computation* **2021** *17* (6), 3554-357
2. "GROMACS: High performance molecular simulations through multi-level parallelism from laptops to supercomputers", M.J. Abraham, T. Murtola, R. Schulz, S. Páll, J.C. Smith, B. Hess, and E. Lindahl, *SoftwareX* **2015**, 1–2, 19–25.
3. "Robust Atomistic Modeling of Materials, Organometallic, and Biochemical Systems" S. Spicher, S. Grimme, *Angew. Chem. Int. Ed.* **2020**, *59*, 15665.
4. "Rationale for mixing exact exchange with density functional approximations" John P. Perdew, Matthias Ernzerhof, Kieron Burke *J. Chem. Phys.* **1976**, 105 (22), 9982
5. Gaussian 16, Revision B.01, M. J. Frisch, G. W. Trucks, H. B. Schlegel, G. E. Scuseria, M. A. Robb, J. R. Cheeseman, G. Scalmani, V. Barone, G. A. Petersson, H. Nakatsuji, X. Li, M. Caricato, A. V. Marenich, J. Bloino, B. G. Janesko, R. Gomperts, B. Mennucci, H. P. Hratchian, J. V. Ortiz, A. F. Izmaylov, J. L. Sonnenberg, D. Williams-Young, F. Ding, F. Lipparini, F. Egidi, J. Goings, B. Peng, A. Petrone, T. Henderson, D. Ranasinghe, V. G. Zakrzewski, J. Gao, N. Rega, G. Zheng, W. Liang, M. Hada, M. Ehara, K. Toyota, R. Fukuda, J. Hasegawa, M. Ishida, T. Nakajima, Y. Honda, O. Kitao, H. Nakai, T. Vreven, K. Throssell, J. A. Montgomery, Jr., J. E. Peralta, F. Ogliaro, M. J. Bearpark, J. J. Heyd, E. N. Brothers, K. N. Kudin, V. N. Staroverov, T. A. Keith, R. Kobayashi, J. Normand, K. Raghavachari, A. P. Rendell, J. C. Burant, S. S. Iyengar, J. Tomasi, M. Cossi, J. M. Millam, M. Klene, C. Adamo, R. Cammi, J. W. Ochterski, R. L. Martin, K. Morokuma, O. Farkas, J. B. Foresman, and D. J. Fox, Gaussian, Inc., Wallingford CT, **2016**.
6. "Effect of the damping function in dispersion corrected density functional theory", Grimme, S., Ehrlich, S. and Goerigk, L. *J. Comput. Chem.* **2011**, 32: 1456-1465.
7. "Anharmonic vibrational properties by a fully automated second-order perturbative approach" V. Baronea, *J. Chem. Phys.* **2005**, 122, 014108
8. "Unravelling the structure of glycosyl cations via cold-ion infrared spectroscopy" Mucha, E., Marianski, M., Xu, FF. *et al.* . *Nat. Commun.* **2018**, 9, 4174
9. "Remote Participation during Glycosylation Reactions of Galactose Building Blocks: Direct Evidence from Cryogenic Vibrational Spectroscopy" M. Marianski, E. Mucha, K. Greis, S. Moon, A. Pardo, C. Kirschbaum, D. A. Thomas, G. Meijer, G. von Helden, K. Gilmore, P. H. Seeberger, K. Pagel, *Angew. Chem. Int. Ed.* **2020**, *59*, 6166.